AGU ADVANCING EARTH AND SPACE SCIENCE

Earth's Future

REVIEW ARTICLE
10.1029/2023EF003679

# Solar Geoengineering in the Polar Regions: A Review

**Alistair Duffey[1], Peter Irvine[2], Michel Tsamados[1], and Julienne Stroeve[1,3,4]**

[1]Centre for Polar Observation and Modelling, Earth Sciences, UCL, London, UK, [2]Earth Sciences, UCL, London, UK, [3]Centre for Earth Observation Science, University of Manitoba, Winnipeg, MB, Canada, [4]National Snow and Ice Data Center, Cooperative Institute for Research in Environmental Sciences, University of Colorado, Boulder, CO, USA

**Key Points:**

- Global solar geoengineering, if technically feasible, would likely reduce the rapid climate change ongoing in the Arctic and Antarctic
- Targeted solar geoengineering strategies would be needed to avoid residual warming in the polar regions
- No truly localized polar geoengineering proposal has been shown viable for restoring climate on a pan-Arctic or Antarctic scale

**Supporting Information:**

Supporting Information may be found in the online version of this article.

**Correspondence to:**

A. Duffey,
alistair.duffey.21@ucl.ac.uk

**Citation:**

Duffey, A., Irvine, P., Tsamados, M., & Stroeve, J. (2023). Solar geoengineering in the polar regions: A review. *Earth's Future*, *11*, e2023EF003679. https://doi.org/10.1029/2023EF003679

Received 21 MAR 2023
Accepted 20 MAY 2023

**Author Contributions:**

**Conceptualization:** Alistair Duffey, Peter Irvine, Michel Tsamados
**Investigation:** Alistair Duffey
**Methodology:** Alistair Duffey, Peter Irvine
**Supervision:** Peter Irvine, Michel Tsamados, Julienne Stroeve
**Writing – original draft:** Alistair Duffey
**Writing – review & editing:** Alistair Duffey, Peter Irvine, Michel Tsamados, Julienne Stroeve



**Abstract** Solar geoengineering refers to proposals, including stratospheric aerosol injection (SAI), to slow or reverse climate change by reflecting away incoming sunlight. The rapid changes ongoing in the Arctic and Antarctic, and the risk of exceeding tipping points in the cryosphere within decades, make limiting such changes a plausible objective of solar geoengineering. Here, we review the impacts of SAI on polar climate and cryosphere, including the dependence of these impacts on the latitude(s) of injection, and make recommendations for future research directions. SAI would cool the polar regions and reduce many changes in polar climate under future warming scenarios. Some under-cooling of the polar regions relative to the global mean is expected under SAI without high latitude injection, due to latitudinal variation in insolation and $CO_2$ forcing, the forcing dependence of the polar lapse rate feedback, and altered atmospheric dynamics. There are also potential limitations in the effectiveness of SAI to arrest changes in winter-time polar climate and to prevent sea-level rise from the Antarctic ice sheet. Finally, we also review the prospects for three other solar geoengineering proposals targeting the poles: marine cloud brightening, cirrus cloud thinning, and sea-ice albedo modification. Sea-ice albedo modification appears unlikely to be viable on pan-Arctic or Antarctic scales. Whether marine cloud brightening or cirrus cloud thinning would be effective in the polar regions remains uncertain. Solar geoengineering is an increasingly prominent proposal and a robust understanding of its consequences in the polar regions is needed to inform climate policy in the coming decades.

**Plain Language Summary** It may be possible to temporarily limit the impacts of climate change by reflecting away part of the incoming sunlight reaching the Earth. Ideas for how to do this are termed solar geoengineering. The Arctic and Antarctic are warming rapidly and change in these regions contributes to serious problems caused by climate change, such as global sea level rise. Additionally, we may exceed warming thresholds within several decades beyond which changes in the polar climate system become self-perpetuating. As a result the Arctic and Antarctic are potential regional targets of solar geoengineering. In this study we review for the first time the evidence on how various forms of solar geoengineering would impact the Arctic and Antarctic. We find that while solar geoengineering is less effective in the polar regions, which receive less sunlight to reflect away than the lower latitudes, global deployment could meaningfully reduce all the projected changes due to climate change which we assess. The potential effectiveness of local polar schemes, which would aim to change the energy balance only over the Arctic or Antarctic, remains very uncertain. The limited evidence we have suggests such options would be insufficient to prevent regional change under high emissions scenarios.

## 1. Introduction

Rapid and deep reductions in greenhouse gas emissions are necessary to limit the harm to people around the world expected due to climate change over the 21st Century (IPCC, 2022). However, increasing awareness of the failure of global climate policy to bring about the rate of change in the global economic system necessary to meet the 1.5°C global warming level (van de Ven et al., 2023; UN Environment Programme, 2022; Sognnaes et al., 2021) identified in the Paris Agreement (UNFCCC, 2015) has led some to consider the use of solar geoengineering—the deliberate cooling of the planet by reflecting away incoming sunlight—to reduce these harms (National Academies of Sciences, Engineering, and Medicine, 2021). Such consideration has been made more urgent by the large changes in the climate system already observed at 1.1°C of warming (Gulev et al., 2021), changes which are particularly stark in the polar regions (Pörtner et al., 2019). Recent work has demonstrated the significant risk that several cryospheric tipping elements in the Earth system, including abrupt boreal permafrost thaw, and collapse of the West Antarctic Ice Sheet, may become active at global temperatures below the Paris

agreement target of 2°C warming (Armstrong McKay et al., 2022; Lenton et al., 2019). The potential for such near-term tipping points provides an additional urgency to consideration of targeted geoengineering in the polar regions, and to developing our understanding of the impacts of global geoengineering on the polar regions.

In the four decades since regular satellite observations of the Arctic began, the region has warmed nearly four times faster than the global average (Rantanen et al., 2022), the sea-ice extent in late Summer has declined by approximately 50% (Fetterer et al., 2017, updated 2023), and the sea-ice volume by perhaps 75% (Kwok & Rothrock, 2009; Notz & Stroeve, 2018). On land, snow cover extent and duration is falling rapidly across the Arctic (Mudryk et al., 2020), and permafrost temperatures are increasing globally, by around 0.3°C over the last 20 years (Biskaborn et al., 2019). The Greenland ice sheet is losing mass at an accelerating rate (Bamber et al., 2018; The IMBIE Team, 2020), and may pass a tipping point into decline on millennial timescales at temperatures below 2°C global warming (Pattyn et al., 2018).

Antarctic sea ice reached its lowest extent on record in 2022 (Fetterer et al., 2017, updated 2023). Currently, the summer Antarctic sea ice is tracking once again at record low values in early 2023, leading to speculation that a signal from anthropogenic warming in Antarctic sea ice cover is finally emerging, amongst the noise of large inter-annual variability. Regionally, strong amplification of warming and sea-ice loss is observed in the Antarctic Peninsula (Hoegh-Guldberg et al., 2018; Siegert et al., 2019) and parts of the vulnerable West Antarctic Ice Sheet may be approaching, or even have already passed, tipping points leading to collapse on multi-century to millennial timescales (Armstrong McKay et al., 2022; Joughin et al., 2014).

These dramatic changes are expected to continue over the coming decades. Projections from the CMIP6 model ensemble find that it is likely already too late to save Arctic summer sea ice using emissions reductions alone (Notz & Community, 2020); Ice-free summers are predicted by the majority of models under even the IPCC's lowest emissions scenario, SSP1-1.9, which reaches net zero around 2050 (Notz & Community, 2020). Extrapolating the approximately linear relationship between Arctic sea-ice and cumulative $CO_2$ emissions, ice-free summers would be expected after around 20 further years of current annual emissions (Notz & Stroeve, 2018).

Change in the polar regions does not remain isolated there. As the coverage of reflective ice and snow decreases, more solar radiation is absorbed, further increasing global temperatures (Pistone et al., 2014). The release of methane and $CO_2$ from thawing permafrost adds substantially to the global burden of greenhouse gases (Comyn-Platt et al., 2018; MacDougall et al., 2015; Schuur et al., 2022); Gasser et al. (2018) estimate that $CO_2$ and $CH_4$ emissions from permafrost thaw would use up approximately 10% of the remaining emissions budget, measured from 2017, to remain under 2°C warming. Polar change also contributes to global sea level rise. Mass loss from the ice sheets is the most uncertain contribution to projections of sea level rise (Edwards et al., 2021), and dominates sea level rise projections on the timescale of several centuries (Fox-Kemper et al., 2021). Sea level rise exceeding 1 m by 2100, while unlikely, is plausible if widespread onset of dynamic ice sheet instabilities occurs (DeConto & Pollard, 2016). Finally, rapid Arctic warming and the loss of sea-ice may increase extreme weather in the mid-latitudes (Cohen et al., 2014; Horton et al., 2015) through changes to the dynamics of the jet-stream and high-latitude modes of variability (De & Wu, 2019; Francis & Vavrus, 2012; Overland et al., 2016).

Solar geoengineering, or Solar Radiation Modification (SRM) refers to a set of proposed techniques by which global warming due to anthropogenic GHG emissions could be offset or partially offset by making the earth more reflective and so decreasing the solar energy absorbed (Shepherd, 2009). Various methods have been proposed for achieving SRM. Stratospheric Aerosol Injection (SAI) is the leading proposal, but others include marine cloud brightening and sea-ice surface albedo modification. Cirrus cloud thinning is not technically SRM since it would alter the Earth's outgoing longwave radiation rather than the incoming solar radiation, but it shares various features with SRM so will be discussed in that context. While most research on SRM has focused on global applications, all the options listed above could be used in a regionally targeted manner, with at least some control of the latitudinal profile of cooling applied. Motivations for using this kind of targeted polar geoengineering which have been proposed in the literature include: to counteract the rapid climate change ongoing in the Arctic (Caldeira & Wood, 2008; MacCracken, 2016; Moore et al., 2014; Tilmes et al., 2014); to prevent the onset of positive temperature feedbacks (Desch et al., 2017; Jackson et al., 2015); and to reduce risks of large and rapid sea level rise arising from loss of ice sheets in Greenland and Antarctica (Irvine et al., 2018). It has also been suggested that using high latitude injection as part of a global SAI strategy might unlock new regions of the "design space" for SAI, and thus give greater control of the resulting climate (Ban-Weiss & Caldeira, 2010; Kravitz et al., 2016; Y. Zhang et al., 2022).

In this review, we draw on multiple lines of evidence to assess how SAI is expected to impact polar climate. In Section 2, we introduce solar geoengineering in more detail. In Section 3, we assess the impact of global SAI scenarios on the polar regions. We first consider the temperature response in the high latitudes, and the reasons for polar under-cooling and a suppressed seasonal cycle which are observed under low-latitude SAI. We then assess in turn the impacts of SAI on sea-ice, hydrology, permafrost, polar contributions to sea level rise, and ocean heat transport in the high latitudes. Next, in Section 4, we assess how these impacts on climate differ when SAI is instead targeted to the polar regions, using injection at high latitude. Finally, in Section 5, we briefly review methods other than SAI by which geoengineering could be enacted in the polar regions. Sections 6 and 7 summarize and propose future research directions.

## 2. Solar Geoengineering

Stratospheric aerosol injection (SAI) is a proposed technique to mimic the cooling effects of volcanic eruptions by injecting aerosols or their precursors into the stratosphere, where they would scatter some incoming shortwave radiation (Shepherd, 2009). SAI is generally considered the most plausible geoengineering method, at least for global applications, because of its low cost, plausible near-term readiness, large possible climate forcing, and relative safety (Shepherd, 2009). Observations of past volcanic eruptions give evidence of the effectiveness of injecting sulfate aerosols and the risk of serious unforeseen consequences (Halstead, 2018). Various methods have been proposed for injecting the aerosols, including balloons, airships and artillery, but the most cost-effective option would likely be a fleet of custom-built aircraft (Moriyama et al., 2017). SAI is likely to be inexpensive compared to the cost of emissions mitigation and well within the budgets of large states; cost estimates are typically in the low tens of billions per year (Moriyama et al., 2017; Smith, 2020).

The stratospheric circulation would spread any injected aerosols rapidly across all longitudes (e.g., Robock et al., 2008) and so SAI cooling cannot in general be limited to a particular region, unlike in the case of marine cloud brightening (e.g., Latham et al., 2014). However, the choice of injection location and timing would give some control over the resulting latitudinal profile of cooling under SAI (Kravitz et al., 2016). As a result, there is the potential for SAI deployment to control more than one feature of the climate system simultaneously, for example, global mean temperature and equator-to-pole temperature gradient (Kravitz et al., 2016; Y. Zhang et al., 2022). Stratospheric circulation tends to push aerosols toward the poles (Kravitz et al., 2017; Robock et al., 2008), so generating aerosol burdens which peak at the poles by using high latitude injection is likely possible, as is seen in the simulations of W. R. Lee et al. (2021b). Simulations of this type of "polar" SAI deployment are examined in Section 4. The degree of this localization should not be overstated. With injection at latitudes poleward of 60°N, various studies using different models have found that the resulting aerosol burdens extend southwards into the Northern Hemisphere tropics (Dai et al., 2018; Jackson et al., 2015; W. R. Lee et al., 2021b; Robock et al., 2008).

It has been suggested (e.g., W. R. Lee et al., 2021b) that since the tropopause in the polar regions is typically below altitudes reached by commercial aircraft, sub-polar injection could use existing aircraft designs. While this is true, Smith et al. (2022) argue it would be more economical to develop purpose-built aircraft, as has also been reported for lower latitude injection strategies (Moriyama et al., 2017; Smith, 2020). Nevertheless, the reduced altitude requirements for injection at higher latitudes would facilitate larger payloads and thus fewer required planes and flights to achieve a given injection mass (Smith et al., 2022). A further consideration for the logistics of high latitude aerosol injection is the limited inhabited land at high latitudes in the Southern hemisphere. Other than Antarctic research stations, Southern Patagonia and the Falkland Islands are the only permanently inhabited land South of 47°S, and the Southernmost airfields in Patagonia are at around 54°S (Smith et al., 2022). In their assessment of an SAI strategy targeting 60°North and South deployment, Smith et al. (2022) elect to limit the Southern hemisphere injection to 54°S to keep the length of each flight to a minimum (it is assumed that these existing Patagonian airfields are used as bases). No study has assessed the feasibility or cost differential for delivering aerosols to the stratosphere at higher Southern latitudes.

Non-SAI proposals for polar geoengineering, discussed in Section 5, include marine cloud brightening (Kravitz et al., 2014), sea-ice surface albedo modification (Field et al., 2018; Webster & Warren, 2022), cirrus cloud thinning (Storelvmo & Herger, 2014), and thickening Arctic sea ice by pumping water onto it (Desch et al., 2017). There are also proposals for mechanically arresting dynamic mass-loss from ice sheets in Antarctica and Greenland (Moore et al., 2018), but an assessment of such methods falls outside the scope of this review.

10.1029/2023EF003679

**Table 1**
*Polar SRM Modeling Studies Referenced in This Review*

| Reference | Forcing type | Latitude | Model type | Experiment description |
|---|---|---|---|---|
| W. R. Lee et al. (2023) | $SO_2$ injection | 60°N | ESM-CC (CESM2-WACCM6) | Two Arctic SAI scenarios which target holding September sea-ice extent at 2010 or 2030 levels |
| W. R. Lee et al. (2021b) | $SO_2$ injection | 60°, 67.5°, and 75°N | ESM-CC (CESM1-WACCM) | Six Arctic SAI scenarios with varying injection latitude and timing |
| Jackson et al. (2015) | $SO_2$ injection | 79°N | ESM (HadGEM2-CCS) | Spring-time injection over Svalbard to hold September sea-ice area at it's 1970–2005 value under RCP4.5 |
| Nalam et al. (2018) | Prescribed aerosols | >50°N/S | AGCM (CAM4) | Monsoon region precipitation assessed under Arctic only, polar, and global SAI |
| Sun et al. (2020) | Prescribed aerosols | 63°N | AOGCM (CESM-CAM4) | An assessment of monsoon region precipitation under tropical and Arctic injection scenarios |
| Robock et al. (2008) | $SO_2$ injection | 68°N | AOGCM (GISS) | A 3-member ensemble modeling SAI with Arctic or tropical injection of 3 Mt $SO_2$ per year |
| Tilmes et al. (2014) | Insolation reduction | >60°N, >70°N | ESM (CCSM4) | Five experiments reducing Arctic insolation by 3%–13% under RCP8.5 |
| Caldeira and Wood (2008) | Insolation reduction | >61°N, >71°N | ESM (CAM3) | Arctic insolation reduced by 10%–50% under a doubled $CO_2$ scenario |
| MacCracken et al. (2013) | Insolation reduction | >51°, >61°, >71°N/S | ESM (CAM3) | Nine experiments with polar insolation reduced by 6%–25% in one or both hemispheres |

*Note.* Where injection is modeled, the "Latitude" column shows the latitude(s) of injection. Where aerosols are prescribed or insolation is reduced, the latitude(s) given are the region of the applied forcing, except in the case of Sun et al. (2020), where the injection latitude equivalent to the prescribed burden is given. Where studies model both high latitude and low latitude/global SAI scenarios, only the latitude(s) associated with the former are shown. In the "Model" column, AGCM indicates an atmosphere-only general circulation model (GCM), AOGCM a coupled atmosphere-ocean GCM, ESM an Earth System Model, that is, an AOGCM with additional components such as land surface and sea ice models, and ESM-CC indicates an Earth System Model with coupled chemistry.

## 3. Impacts of Global SAI on the Polar Regions

### 3.1. SAI in Climate Models

In this section, we assess the impacts of global SAI on polar climate and the cryosphere. No large-scale field testing of SAI has been carried out. Indeed, tests of the climate response to SAI, such as its impact on global surface temperature or precipitation, would need to be of a forcing magnitude and time-scale large enough (e.g., >0.1 W/m$^2$ over decades (MacMynowski et al., 2011)) to be difficult to distinguish from deployment (Lenferna et al., 2017; MacMartin & Kravitz, 2019). While the record of past climate response to volcanic eruptions provides important evidence, it is an imperfect proxy for deliberate, sustained SAI (National Academies of Sciences, Engineering, and Medicine, 2021). As such, our assessment draws heavily on modeling, mostly in earth system models and general circulation models. These modeling studies typically simulate SAI by adding aerosols or their precursors to the model stratosphere, or in some cases, by prescribing an aerosol optical depth field derived from another model. A list of global geoengineering scenarios referenced in this review is given in Table S1 in Supporting Information S1 and a list of studies modeling polar SAI, referred to in Section 4, is given in Table 1. We will also refer throughout to several solar geoengineering scenarios simulated by multiple modeling centres under the Geoengineering Model Intercomparison Project, GeoMIP (Kravitz et al., 2011, 2015). These GeoMIP simulations are a vital means of assessing the robustness of findings in the context of large inter-model differences (Visioni et al., 2023).

As well as SAI simulations, we also draw on evidence from studies modeling solar dimming, that is, reducing insolation, as an incomplete proxy for the impacts of SAI. Solar dimming simulations can capture the difference between the climate system response to shortwave and longwave radiative forcings, which is expected to be an important contributor to differences in surface climate under SAI (Ammann et al., 2010; Kravitz et al., 2013). But they exclude various other features of SAI, including the seasonal and spatial variability of aerosol distributions, stratospheric heating via infrared absorption by aerosols and changes to stratospheric chemistry (Visioni, MacMartin, & Kravitz, 2021). Stratospheric heating, which is expected as a side-effect of SAI using sulfate aerosols, would cause changes in stratospheric dynamics (Aquila et al., 2014) which impact surface climate via changes in atmospheric circulation (A. Jones et al., 2021; Simpson et al., 2019). These solar dimming simulations are needed, in part, because of the relative paucity of SAI simulations. Comparing the modeled response to solar dimming and simulated aerosol injection can also be a useful means of diagnosing the causes of modeled surface climate changes under SAI (e.g., A. Jones et al., 2021).

SAI could be deployed in many ways. The altitude, particle species, and, in particular, latitude and season of injection would all affect the impact of SAI on polar climate (Visioni et al., 2020; Y. Zhang et al., 2022). In this review we consider the impacts on polar climate of two categories of SAI separately; (a) "global SAI," in which aerosols are injected in the tropics or subtropics (at or equatorward of 30°) or uniformly across all latitudes, and (b) "polar SAI," in which aerosols are injected in the sub-polar or polar regions (at or poleward of 60°) only. In recent years, various studies, beginning with Kravitz et al. (2017), have modeled more complex SAI deployments in which injections at several latitudes are varied in response to the

evolving simulated climate. These deployments make use of feedback algorithms, altering injections year-by-year to control features of the modeled climate system. The Geoengineering Large Ensemble, GLENS (Tilmes et al., 2018), is an example of this type of simulation. GLENS is a 20-member ensemble of SAI simulations in the Community Earth System Model (CESM), with varying injection magnitude at ±15°N/S and ±30°N/S to control three features of the climate: global mean temperature, inter-hemispheric temperature gradient, and the equator-to-pole temperature gradient. Here we class these deployments as "global."

### 3.2. Temperature of the Polar Regions

There is multi-model consensus that SAI would reduce both Arctic and Antarctic annual-mean temperatures (Berdahl et al., 2014; Visioni, MacMartin, Kravitz, Boucher, et al., 2021). However, for a given global mean surface temperature cooling, many SAI simulations show an over-cooling of the tropics and under-cooling of the polar regions, particularly in the Northern Hemisphere (Berdahl et al., 2014; Govindasamy & Caldeira, 2000; Visioni, MacMartin, Kravitz, Boucher, et al., 2021). This means that while SAI is highly effective at reducing temperature changes, there is, in general, a greater Arctic amplification of warming modeled under SAI at a speficic global warming level as compared to a world at the same warming level under GHG forcing only (Berdahl et al., 2014; Ridley & Blockley, 2018). This pattern has been found under simulations of solar dimming (Govindasamy & Caldeira, 2000; Henry & Merlis, 2020; Kravitz et al., 2013; MacMartin et al., 2013; Tilmes et al., 2018), SAI using tropical injection (Berdahl et al., 2014; Visioni, MacMartin, Kravitz, Boucher, et al., 2021; Yu et al., 2015), and SAI using a spatially uniform aerosol optical depth (Ridley & Blockley, 2018). However, SAI simulations with sufficient injection at off-equatorial latitudes have been found to strongly reduce this effect (Kravitz et al., 2017; Richter et al., 2022).

The annual-mean radiative forcing from a uniform decrease in insolation has greater meridional gradient than the longwave forcing from increased greenhouse gas concentrations (Govindasamy et al., 2003; Jiang et al., 2019). This difference explains part of the under-cooling of the polar regions seen under solar dimming scenarios, such as the GeoMIP scenario G1 (Henry & Merlis, 2020; Kravitz et al., 2013). A second, potentially larger, contribution to this polar under-cooling arises due to the differing vertical profile of temperature change induced by solar forcing versus $CO_2$ forcing. In the tropics, convection returns the tropospheric lapse rate toward the moist adiabat, meaning lapse rate changes with temperature are approximately independent of the forcing type (Xu & Emanuel, 1989). However, in the polar regions, where the troposphere is typically stable against moist convection, this is not the case (Cronin & Jansen, 2016; Henry & Merlis, 2020). Warming from increased $CO_2$ is strongly trapped near the surface in the polar regions, giving rise to the positive lapse rate feedback which is a major contributor to Arctic amplification (Goosse et al., 2018; Pithan & Mauritsen, 2014). The magnitude of this positive lapse rate feedback is not independent of the type of forcing; the cooling from reduced insolation is more vertically homogenous and so the net effect of increased $CO_2$ and reduced insolation is a more positive lapse rate feedback and residual surface warming, even with zero top of atmosphere forcing (Henry & Merlis, 2020). We note that Pithan and Mauritsen (2014) use top-of-atmosphere fluxes to decompose feedback contributions to Arctic amplification. This method does not account for interactions between radiative feedbacks and energy transport (Russotto & Biasutti, 2020). Several recent studies that do include such interactions find somewhat altered contributions, including a positive rather than negative contribution to Arctic amplification from water vapor feedback when its impacts on energy transport are inlcluded (Henry et al., 2021; Russotto & Biasutti, 2020).

A third contribution to polar under-cooling arises from the latitudinal profile of aerosol optical depth. SAI scenarios with injection near the Equator simulate aerosol concentrations which are lower at the poles than in the tropics (Figure 1a). The importance of this contribution to under-cooling of the high latitudes is shown by Kravitz et al. (2019) through their comparison of surface temperature under equatorial injection against a scenario (GLENS, see Section 3.1) which controls injection latitudes in order to restore the equator-to-pole temperature gradient. This latter scenario results in a bimodal aerosol optical depth distribution which peaks in the mid-latitudes and strongly reduces the under-cooling of the high latitudes relative to the equatorial injection case (Kravitz et al., 2019). While some polar under-cooling remains in this scenario, the change in equator-to-pole temperature gradient is reduced by well over two thirds relative to the background scenario RCP8.5 (Tilmes et al., 2018). Whether under-cooling of the poles under SAI could be completely avoided under deployments with greater injection at higher latitudes is discussed in Section 4.

SAI might be expected to suppress the seasonal cycle at high latitudes because the radiative forcing from reflecting incoming shortwave radiation is more strongly seasonal than the forcing due to GHG increases (Govindasamy & Caldeira, 2000; Govindasamy et al., 2003; Jiang et al., 2019; Lunt et al., 2008). SAI radiative forcing at high

10.1029/2023EF003679

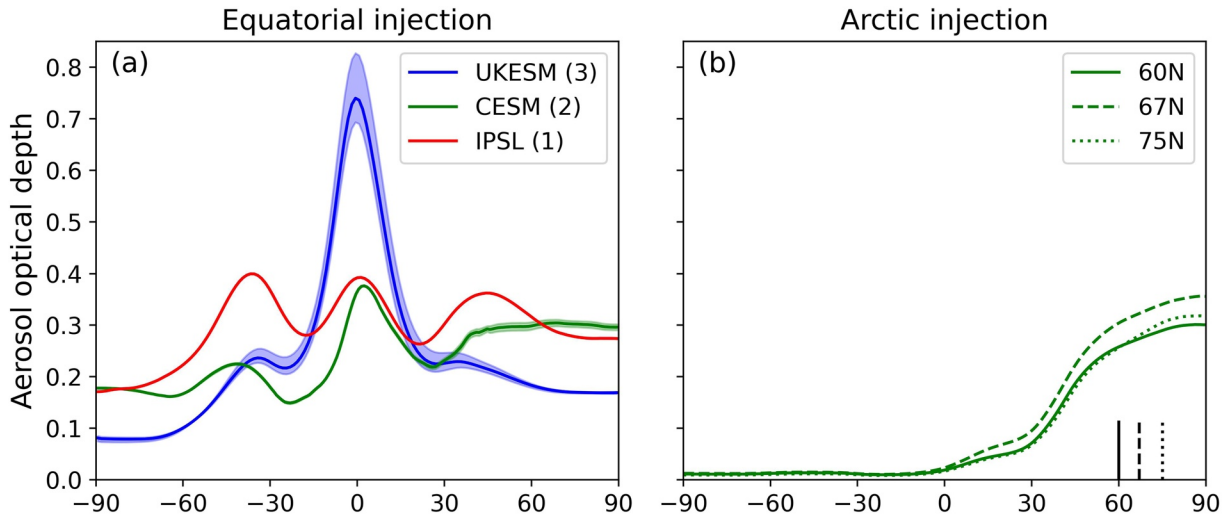


**Figure 1.** Zonal mean stratospheric aerosol optical depth (AOD) under equatorial and Arctic injection. (a) AOD under the GeoMIP scenario G6sulfur. In UKESM1-0-LL and IPSL-CM6A-LR aerosols are injected uniformly between 10°S and 10°N, and at a single longitude, while in CESM2-WACCM injection is on the equator. (b) Annual mean AOD in the model CESM1-WACCM under Arctic injection of 12 Tg $SO_2$ per year, with injection at approximately 15 km altitude and limited to the months of March, April and May. Black vertical lines show the latitude of injection in each of the three cases. In (a) we plot AOD for the three earth system models which have simulated aerosol transport under the G6sulfur scenario. The magnitude of injection varies between models. Where multiple ensemble members are available shading indicates the ensemble spread and the line indicates the ensemble mean. The number of ensemble members available in each case is given in brackets. The stratospheric aerosol optical depth output was not available for CESM2-WACCM so in this case we show the difference in whole atmosphere aerosol optical depth between the G6sulfur scenario and the background scenario SSP5-8.5, which approximates the stratospheric aerosol optical depth.

latitudes would peak in local summer, when insolation is largest, and would be negligible during the winter when insolation is unimportant to the polar energy budget (Serreze et al., 2007). However, despite the lack of sunlight, SAI is still modeled to reduce polar temperatures during winter (Kravitz et al., 2019). Radiative forcing during the sunlit months has a large impact on winter-time Arctic temperatures because it changes ocean heat uptake, which is released back to the atmosphere in winter (Bintanja & Krikken, 2016). Additionally, cooling at lower latitudes can reduce winter-time poleward atmospheric and oceanic heat fluxes (Nalam et al., 2018). Overall, taking the Arctic region as a whole, the net effect of these different contributions is a reduction in the amplitude of the Arctic seasonal temperature cycle under SAI due to winter-time under-cooling, relative to a world at the target global mean temperature without SAI (Jiang et al., 2019). In some regions, this modeled reduction is as large as 40% (Jiang et al., 2019).

Regionally, a dipole-like pattern of winter-time cooling in the Arctic has been modeled under several SAI scenarios, with under-cooling (i.e., residual warming compared to a baseline state at the same global mean temperature under GHG forcing only) over Northern Eurasia, Greenland, and most of the Eastern Arctic Ocean, and over-cooling over the Canadian Archipelago and Western Arctic Ocean (Banerjee et al., 2021; Jiang et al., 2019; A. Jones et al., 2021; Kravitz et al., 2019). The cause of this pattern appears to be, at least in part, that infra-red absorption by sulfate aerosols warms the lower stratosphere, particularly in the tropics, resulting in changes in atmospheric circulation which are associated with winter-time surface warming over Northern Eurasia (Banerjee et al., 2021; A. Jones et al., 2021). Volcanic eruptions provide some real-world verification for this finding. Winter-time Eurasian warming has been observed (Shindell et al., 2004; Wunderlich & Mitchell, 2017) and modeled (Pauling et al., 2021) following large volcanic eruptions, although recent evidence suggests that these observed winter-warming events following eruptions may have been due to natural variability rather than the volcanic forcing, as a significantly larger stratospheric aerosol loading is required than was present under these eruptions for the signal to be detectable (Polvani et al., 2019).

The proposed mechanism by which SAI causes winter-time warming in Northern Eurasia is that stratospheric warming due to near-infrared absorption by aerosols in the tropics increases the equator-to-pole temperature gradient in the stratosphere, especially in winter. This results in a strengthened polar vortex leading to a more positive-NAO like tropospheric circulation (Banerjee et al., 2021; Thompson & Wallace, 2001), which is associated with winter warming over Northern Eurasia (A. Jones et al., 2021; Robock, 2000). In contrast to the

wintertime warming of Northern Eurasia, the stratospheric heating under SAI has been associated with a wintertime cooling over much of North America (A. Jones et al., 2021) so may contribute to the increase in amplitude of seasonal temperature cycle under SAI in the Canadian archipelago reported by Jiang et al. (2019).

### 3.3. Arctic Sea Ice

Temperature is the main driver of variation in Arctic sea-ice on long timescales (Notz & Stroeve, 2018) and so to first order it is expected that global SAI would reduce the loss of sea ice under future warming. Such restoration of sea ice by SAI has been demonstrated in modeling studies, both for solar dimming experiments (Kravitz et al., 2013; Moore et al., 2014) and for aerosol injection (Jiang et al., 2019; A. C. Jones et al., 2018; W. Lee et al., 2020). Variation in sea-ice is also driven by atmospheric and oceanic circulation (Mallett et al., 2021; Stroeve et al., 2011), local radiative equilibrium (Notz & Stroeve, 2016) and poleward latent heat fluxes (Yang & Magnusdottir, 2018). As such, SAI may impact sea ice independently of local temperature.

Under solar dimming scenarios, there is multi-model consensus that both Arctic and Antarctic sea-ice extents can be held at close to their present-day values (A. Jones et al., 2013; Kravitz et al., 2013), in contrast to large decreases under $CO_2$ increases without geoengineering. Results from modeling of SAI, rather than solar dimming, are more mixed. Under the GeoMIP G3 and G4 scenarios, which model equatorial injection of $SO_2$ to cool the planet by of order 1°C under the RCP4.5 emissions scenario, most CMIP5-era models (4/5 for the G4 scenario and 2/3 for the G3 scenario) see a near-complete loss of Arctic September sea ice (Berdahl et al., 2014). This loss of sea ice occurs despite SAI causing significant ($\gtrsim$50%) reductions in Arctic warming trends (Berdahl et al., 2014). In the G4 scenario, this amounts to an Arctic cooling of approximately 1.5°C relative to RCP4.5 over the period of SAI (2040–2069) (Kashimura et al., 2017). Given a warming relative to pre-industrial of roughly 5°C for this period and scenario in the CMIP5 ensemble (Gutiérrez et al., 2021), this means that the G4 SAI scenario still sees around 3–4°C annual mean Arctic warming relative to pre-industrial. No study has yet assessed the difference in the extent of sea ice under the GeoMIP geoengineering scenarios versus without geoengineering at a given global temperature, so it is not yet clear to what extent the loss of sea ice under the G3 and G4 scenarios is simply a result of insufficient global cooling in these cases. Also, the spread in present-day September sea-ice extent simulated by the models assessed by Berdahl et al. (2014) is large (2–6 million $km^2$), casting some doubt over the robustness of these projections. A quantitative comparison of sea-ice extent under the G6 scenarios against their target SSP2-4.5 could shed light on this question, but has not yet been carried out in the literature.

Several more recent single-model studies (using CMIP6-era models) show greater sea-ice preservation under SAI than that found for the G3 and G4 scenarios, especially under scenarios which include injection away from the equator. A. C. Jones et al. (2018) find that Arctic sea-ice extent is successfully stabilized under globally uniform $SO_2$ injection to hold global temperatures at 1.5°C above pre-industrial. This scenario sees Arctic annual mean warming restricted to approximately 3–5°C above historic at end-century (A. C. Jones et al., 2018). Under the GLENS scenario (see Section 3.1), which holds the equator-to-pole temperature gradients approximately constant in addition to global mean temperature, SAI is effective at restoring both the summer minimum sea-ice and the winter maximum (Jiang et al., 2019; Kravitz et al., 2019). In fact, Arctic sea-ice extent at the September minimum under GLENS is increased by approximately 50% relative to the 2020 baseline (Jiang et al., 2019). This stark increase in summer sea-ice under GLENS contrasts with a reduction in the March maximum extent by 8% relative to the 2020 baseline. A greater restoration of the summer sea-ice minimum than the winter maximum, and consequent dampening of the seasonal sea-ice cycle is a common finding across models and scenarios (Berdahl et al., 2014; Jiang et al., 2019; W. R. Lee et al., 2021b). In the GLENS case, the under-restoration of winter sea-ice extent may be related to the 20% speed-up of the Atlantic Meridional Overturning Circulation (AMOC) observed in this simulation (Fasullo et al., 2018). The AMOC, which transports heat into the North Atlantic, is anti-correlated with lagged sea-ice extent in the control simulations of various general circulation models, particularly in winter (Day et al., 2012; Li et al., 2018; Mahajan et al., 2011), and it has been suggested that a near-term slowdown in the Atlantic heat transport might delay the sea ice in coming decades (Yeager et al., 2015; R. Zhang, 2015). This AMOC speed-up observed under GLENS is, however, not reproduced under SAI scenarios in a later version of the same model (Tilmes et al., 2020), see Section 3.8.

Year-to-year variability of sea-ice volume is driven in large part by atmospheric circulation, including the local wind fields, controlled in part by the Arctic oscillation (AO) (Mallett et al., 2021; Stroeve et al., 2011). A negative phase of the AO is associated with the retention of sea ice through the summer melt season, and therefore a

positive anomaly in September sea ice (Rigor et al., 2002; Stroeve et al., 2011). The negative AO phase promotes an anticyclonic anomaly associated with increased ice transport from the Western to the Eastern Arctic, where ice is more likely to thicken against the Siberian coast (Stroeve et al., 2011). By contrast, a positive AO phase is associated with more formation of thin ice which is prone to melting in the season (Rigor et al., 2002; Stroeve et al., 2011). Tropical lower stratospheric heating occurring as a side-effect of SAI has been associated with driving positive NAO-like atmospheric conditions, which are highly correlated with positive AO conditions (Simpkins, 2021), in two earth system models, UKESM1 and CESM2-WACCM6 (A. Jones et al., 2021). Consequently, it might be assumed that SAI causes a reduction in September sea ice volume via the atmospheric mechanism described above, and that this reduction offsets some part of the increase in volume caused by temperature reduction. It is possible that such a mechanism could contribute to the under-restoration of sea-ice extent in the equatorial injection SAI scenarios described above.

There is little consistency between models in projecting regional sea ice cover changes under SAI (Moore et al., 2014), and so we will not discuss these in detail here. However, relatively small changes in total sea-ice extent can mask large regional changes at the edge of the ice pack, including in regions with indigenous populations whose ways of life will be impacted by such change (Moore et al., 2014). Under the GLENS scenario, at the March maximum, total sea-ice extent falls by only 8% relative to the 2020 baseline, but this includes a large reduction of 30%–60% in sea ice over most of the Barents sea (Jiang et al., 2019). This region of sea ice reduction is colocated with the winter-time Northern Eurasian warming under SAI forced via stratospheric heating, discussed above. The strengthened AMOC in this SAI scenario (Fasullo et al., 2018) may also play a role, since this is associated with reduced Atlantic heat transport across the Barents Sea Opening, which itself is strongly anti-correlated with Barents Sea winter sea-ice extent in the CMIP5 model ensemble (Li et al., 2017).

### 3.4. Antarctic Sea Ice

Turning to Antarctic sea ice, there is less direct modeling evidence available, and no studies assess the response to SAI in detail. Under the solar dimming experiment G1, the March Antarctic summer sea ice minimum is less effectively preserved than the equivalent Arctic summer minimum (Kravitz et al., 2013), although there is little confidence in the ability of the CMIP5-era model projections used here to effectively simulate the Antarctic sea-ice minimum (Turner et al., 2013). In one single-model study, simulations of SAI used to restore global temperature to its twentieth century level under RCP8.5 show an incomplete restoration of Antarctic sea ice, with reduced concentration across most of the marginal ice zone (McCusker et al., 2015). As was the case for Arctic sea ice, greater off-equatorial injection appears to be more effective at restoring Antarctic sea-ice. Jiang et al. (2019) find that the GLENS SAI scenario is effective at restoring Antarctic sea-ice, both at summer minimum and, to a lesser extent, at winter maximum.

Simulations of volcanic eruptions and nuclear winter provide an additional source of evidence for potential SAI impacts on Antarctic sea ice. Antarctic sea ice is less strongly promoted by cooling following volcanic eruptions than Arctic sea ice (Pauling et al., 2021; Zanchettin et al., 2014). An absolute reduction in Antarctic sea-ice extent and volume has even been modeled in the years following simulated forcing from large volcanic eruptions (Zanchettin et al., 2014) and nuclear winter (Coupe et al., 2023), despite global cooling of up to 10°C in these scenarios. This surprising result is associated with increased upwelling and incursions of warmer waters to the sea ice region due to a poleward shift of the polar jet and strengthened westerlies close to the Antarctic coastline, as well as a poleward shift of the Antarctic Circumpolar Current, all of which are attributed to tropical lower stratospheric heating from absorption of insolation by the lofted sulfate aerosols or soot (Coupe et al., 2023; Verona et al., 2019). The soot injected under nuclear winter scenarios is more strongly absorbing than sulfate aerosols, so stratospheric heating and its effects are expected to be amplified in these scenarios relative to volcanic eruptions and SAI (Coupe & Robock, 2021). However, this mechanism has also been simulated under SAI forcing (McCusker et al., 2015). The observational record of Antarctic sea ice is too short to assess the impact of eruptions in the context of large internal variability (Zanchettin et al., 2014), but a suggestive warm anomaly was observed in the Weddel Sea off the Antarctic Peninsula, following the eruption of Mt. Pinatubo (Verona et al., 2019).

Reductions in Antarctic sea ice are not seen under simulations of smaller scale nuclear war (Coupe et al., 2023) and volcanic eruptions (Zanchettin et al., 2014). This suggests a threshold forcing, at least in the nuclear winter case; for cooling magnitudes smaller than this threshold, the increase in sea ice due to global cooling outweighs the reduction in sea ice due to dynamic effects (Coupe et al., 2023). If such a threshold exists for sulfate injection,

the modeled SAI scenarios referenced above simulate forcings below it, since in all cases Antarctic sea ice shows an incomplete restoration by SAI rather than an absolute reduction (Jiang et al., 2019; Kravitz et al., 2013; McCusker et al., 2015).

### 3.5. Permafrost

At large scales, the permafrost area is determined principally by the mean annual surface air temperature, although other factors such as the depth of snow cover and hydrology also have an impact (Burke et al., 2020; Chadburn et al., 2017). SAI reduces mean annual surface temperatures in permafrost regions and so would be expected to reduce the loss of permafrost. There is limited direct modeling of permafrost changes under SAI, but in all cases, SAI is indeed found to reduce GHG emissions from permafrost degradation during its period of deployment (Chen et al., 2023; Chen et al., 2020; Jiang et al., 2019; H. Lee et al., 2019; W. R. Lee et al., 2023; Liu et al., 2023). Two recent multi-model studies assessed the permafrost response under the G6sulfur SAI scenario (Chen et al., 2023; Liu et al., 2023). SAI is found to offset a large fraction of the permafrost carbon loss under SSP5-8.5 (Chen et al., 2023; Liu et al., 2023). However, Chen et al. (2023) show that the winter-time Northern Eurasian warming under this scenario described in Section 3.2 raises annual mean soil temperatures and prevents a full restoration of permafrost extent to that of the target scenario; 39% of baseline permafrost extent is retained under G6sulfur, as compared to 45% under the target scenario SSP2-4.5 (Chen et al., 2023). These findings are broadly in line with the only previous multi-model assessment of permafrost response to SAI (Chen et al., 2020), which found that in the ensemble mean of seven earth system models running the GeoMIP SAI scenario G4, which injects less aerosols than are required to fully offset warming, cumulative $CO_2$ emissions from permafrost melting by 2070 are halved under the geoengineering scenario G4 relative to RCP4.5.

There is some evidence that with greater extra-tropical injection, SAI can more effectively limit permafrost loss. H. Lee et al. (2019) simulate that Northern Hemisphere high latitude soil temperature and permafrost area are maintained approximately constant under an SAI deployment which offset. all high-latitude warming under SSP5-8.5. Similarly, Jiang et al. (2019) report that SAI effectively prevents permafrost loss under the GLENS deployment scenario, which offset. almost all high-latitude warming, with a 5% loss in Arctic annual mean permafrost area, as opposed to an 83% loss by end of century under RCP8.5. The inter-model spread of permafrost carbon release can be several times larger than the spread between scenarios with and without geoengineering (Chen et al., 2020). Also, process models forced by the outputs of earth system models can show qualitatively different permafrost carbon evolution to the earth system models themselves (Liu et al., 2023). As a result, these single-model findings (Jiang et al., 2019; H. Lee et al., 2019; W. R. Lee et al., 2023) should be treated with some caution.

### 3.6. Polar Hydrology

A strong intensification of the hydrological cycle at high latitudes is expected under warming over the 21st century. This is largely energetically driven, that is, increased tropospheric temperatures drive greater radiative cooling to space which balances the local latent heat release from increased precipitation (Pithan & Jung, 2021). Arctic precipitation is expected to increase by 30%–60% under RCP8.5 (Bintanja, 2018; Bintanja & Selten, 2014) and Antarctic precipitation by approximately 50% (Tewari et al., 2022) by 2100. The fraction of this precipitation which falls as rain is also expected to rise, with several regions of the Arctic expected to see more than half of their precipitation fall as rain rather than snow under 1.5°C global warming (McCrystall et al., 2021). Arctic June snow cover declined at over 10% per decade over the last 50 years (Pörtner et al., 2019), predominantly due to increasing surface temperatures. Under SAI, these changes to polar hydrology are expected to reduce. In the GLENS SAI scenario, precipitation (P), evaporation (E), and water availability (P−E) are all reduced relative to RCP8.5 in the high latitudes of both hemispheres (Simpson et al., 2019), and P-E is restored to be statistically indistinguishable from present day in most high northern latitude land regions under the GLENS scenario (Irvine & Keith, 2020). Similarly, in a scenario in which a globally uniform stratospheric aerosol distribution offsets all global-mean warming under a doubling of $CO_2$, Nalam et al. (2018) find changes in polar rainfall and snowfall which are reduced by an order of magnitude relative to the doubled $CO_2$ world. Under a scenario of equatorial injection, there is multi-model consensus that Arctic under-cooling is accompanied by a residual increase in precipitation, although with significant inter-model spread (Visioni, MacMartin, Kravitz, Boucher, et al., 2021). There is no agreement between models on the sign of residual change in Antarctic precipitation relative to the control under equatorial injection (Visioni, MacMartin, Kravitz, Boucher, et al., 2021).

### 3.7. Ice Sheets and Sea Level Rise

Polar regions contribute to sea level rise principally via changes to the amount of ice on land in the form of ice sheets and glaciers. These changes are driven by the sum of surface mass balance (SMB), ocean-driven melt, and dynamic losses at the ice edge (calving). In the case of Greenland, observed ice sheet mass loss is approximately half due to surface melting and half due to dynamic losses (van den Broeke et al., 2009), whereas for the Antarctic, mass loss is mostly due to ocean-driven melt and calving causing the retreat and loss of thickness in outlet glaciers draining the vulnerable West Antarctic Ice Sheet (Bamber et al., 2018). Mass gain occurs via accumulation of precipitation in both cases. Irvine et al. (2018) recently reviewed the literature on the impact of SAI on sea level rise so we give only a brief overview here.

The surface mass balance is the net change in ice mass due to accumulation (from snowfall) and ablation (from evaporation, sublimation and run-off), it does not include ice lost to calving and melting in contact with the ocean. Irvine et al. (2018) argue that solar geoengineering may be more effective at restoring surface mass balance than temperature by around 10%, since SAI reduces downward shortwave radiation, which is an important source of energy for surface melting of ice sheets. In agreement with this, Fettweis et al. (2021) find that solar dimming reduces the surface melt of the Greenland Ice Sheet by ∼6% more than an equivalent global cooling by GHG emissions reduction, due to the reduction in downward shortwave energy flux.

However, in simulations of SAI as opposed to solar dimming, an increase in downward shortwave radiation over Greenland and the high northern latitudes has been found (W. R. Lee et al., 2023; Moore et al., 2019). W. R. Lee et al. (2023) attribute this to a decrease in cloud cover. Under such an increase in downward shortwave flux we might expect SAI to be less effective than emissions mitigation at reducing surface melt at a given temperature. However, outgoing longwave radiation at high northern latitudes is also increased by the reduction in Arctic cloud cover in this simulation (W. R. Lee et al., 2023). Overall, W. R. Lee et al. (2023) find that SMB under their SAI scenario is approximately equal to that during a reference period with statistically identical mean temperature over Greenland. In the only inter-model comparison of Greenland SMB under SAI, Moore et al. (2019) find that the G4 SAI scenario reduces surface run-off relative to the emissions scenario (RCP4.5) from which it branches by only approximately 20% in the multi-model mean of 4 models. This relative ineffectiveness at maintaining SMB appears to be related to an under-cooling of local temperatures over Greenland found in several models in this scenario.

In contrast to Greenland, Antarctic surface mass balance is dominated by accumulation, since it is too cold for significant surface melting (Mottram et al., 2021). Accumulation in Antarctica is expected to increase this century under global warming because of increased snowfall (Lenaerts et al., 2016). The negative contribution to sea level rise from this increased snowfall would decline under SAI, which is expected to suppress high-latitude precipitation increases in both hemispheres (Irvine et al., 2018; Visioni, MacMartin, Kravitz, Boucher, et al., 2021). At present, though, the Antarctic ice sheet mass loss from outlet glaciers, mostly in the West Antarctic, is larger than the mass gain from snowfall (Rignot et al., 2019; The IMBIE Team, 2018), and this is expected to remain the case through the 21st century (Edwards et al., 2021; Seroussi et al., 2020). It is therefore also important to consider the ability of SAI to prevent this "dynamic" ice sheet mass loss. There is deep uncertainty over the drivers of this dynamic mass loss so the impact of SAI is difficult to predict (Irvine et al., 2018). Mass loss from outlet glaciers is facilitated by the thinning and disintegration of ice shelves, which are floating extensions of ice sheets. The loss of ice shelves does not in itself contribute to sea level rise, but removes their buttressing effect and thus increases the rate of mass-loss from marine terminating glaciers, which do contribute to sea level rise (Favier et al., 2014; Pritchard et al., 2012).

Basal melting is an important contributor to the loss of ice shelves and is sensitive to sub-surface ocean temperatures (Pollard et al., 2015). In Antarctica, intrusion of relatively warm circumpolar deep water onto the continental shelf, which can be caused by wind-driven upwelling, is associated with strong basal melting of ice shelves (Thoma et al., 2008). One study has found that SAI fails to fully restore winds over the Southern Ocean, leaving a residual westerly wind stress on the ocean around Antarctica (McCusker et al., 2015). As a result, in this scenario SAI does not prevent the upwelling of warm waters near Antarctic ice shelves, especially around vulnerable glaciers in West Antarctica. This finding, in combination with the reduced accumulation of snow expected under SAI raises the possibility that SAI could have limited ability to arrest, or could even increase, the Antarctic contribution to sea level rise relative to GHG forced warming. The proposed mechanism identified by McCusker et al. (2015) depends on the lower stratospheric meridional temperature gradient induced by SAI. This gradient

is sensitive to both model choice and, more importantly, injection latitude (Bednarz et al., 2022). It is therefore unclear to what extent this limitation in the ability of SAI to prevent basal melt of Antarctic ice shelves is dependent on model choice, and on the injection latitude(s) used in the SAI scenario.

The loss of sea-ice around Antarctica also likely contributes to mass loss from ice shelves and subsequent increased glacier outflow through several mechanisms including increased exposure to ocean swells (Massom et al., 2018), increased solar heating of ocean water and changes to ocean stratification. SAI would at least partially restore Antarctic sea-ice under future warming-driven losses (see Section 3.3), so would reduce this contribution to Antarctic sea-level rise.

Finally, while air temperatures are too cold for significant surface melting over most of the Antarctic ice sheet, this is not the case for all ice shelves (DeConto & Pollard, 2016), the surfaces of which are near sea-level so experience warmer temperatures than the continental Antarctic. Surface melting of ice shelves could cause disintegration via the formation of melt ponds and subsequent hydrofracturing (Bell et al., 2018; DeConto & Pollard, 2016). There is large uncertainty in the importance of this mechanism for ice shelf loss, but it could trigger dynamic instabilities in marine ice sheets (Pollard et al., 2015) causing rapid mass loss and associated large sea level rise this century (DeConto et al., 2021; DeConto & Pollard, 2016). SAI would reduce surface air temperatures over ice shelves and so reduce surface melting. However, if dynamic instabilities of marine ice sheets are already onset, even restoration to pre-industrial climate might be insufficient to prevent further loss (Irvine et al., 2018).

### 3.8. The Arctic Ocean and the Atlantic Meridional Overturning Circulation

There has been little work on the expected changes in ocean circulation caused by SAI, except for several studies on AMOC change. Under the solar dimming scenario, G1, SAI offsets most of the ~40% weakening of AMOC modeled under a quadrupling of $CO_2$, leaving AMOC slightly weakened relative to the control in the multi-model mean (Hong et al., 2017). Similarly, under the SAI scenario G4, which partially offsets warming under RCP4.5, all models show a strengthening of AMOC relative to the warming scenario (Moore et al., 2019; Xie et al., 2022), but in the multi-model mean AMOC is weakened by approximately 8% relative to pre-industrial (Xie et al., 2022). One model out of six simulating this SAI scenario shows a strengthening of AMOC relative to pre-industrial by approximately 5% (Xie et al., 2022).

In contrast to these findings, the GLENS SAI scenario sees a 20% strengthening of AMOC relative to present-day, against a projected 30% weakening under warming without SAI. This AMOC strengthening is associated with large residual ocean warming under GLENS relative to present-day in the Arctic and around South Greenland (Fasullo et al., 2018). Residual ocean warming is also observed in the Antarctic under this scenario. The model used for the GLENS simulations (CESM1-WACCM) is not one of those simulating G4 assessed by Xie et al. (2022) or Moore et al. (2019), and the aerosol distribution under GLENS is very different to that under G4 (see Section 3.1). A more recent version of the same model (CESM2-WACCM6) does not reproduce these AMOC changes (Tilmes et al., 2020). Under a similar SAI scenario to GLENS, this model version finds that SAI reduces the slowdown of AMOC simulated under GHG-forced warming (Tilmes et al., 2020), broadly in line with the projections under G4 discussed above. Changes in ocean circulation, including AMOC, forced by SAI remain an important poorly constrained source of uncertainty in our understanding the impacts of SAI on the polar regions.

## 4. Arctic and Antarctic Climate Under Polar SAI

In this section, we examine the local and global impacts of SAI with injection at latitudes poleward of ~60°, hereafter referred to as "polar SAI.".The earliest study modeling polar SAI was conducted by Robock et al. (2008). Since that publication, we are aware of five further studies which simulate polar SAI in an earth system model or general circulation model, see Table 1. In addition, several studies have modeled the response to reduced insolation in high latitude regions, as a simplified proxy for SAI (Caldeira & Wood, 2008; MacCracken et al., 2013; Tilmes et al., 2014). Two studies have modeled scenarios in which Arctic SAI or solar dimming is balanced by Antarctic deployment (MacCracken et al., 2013; Nalam et al., 2018). We first consider the spatial distribution of stratospheric aerosols which is expected following injection at high latitudes. We then assess efficiency of polar SAI at reducing temperature both locally in the Arctic and Antarctic, and globally, on a °C per Tg sulfate basis. Finally, impacts of polar SAI on sea-ice, polar hydrology, and tropical precipitation, are discussed.

10.1029/2023EF003679

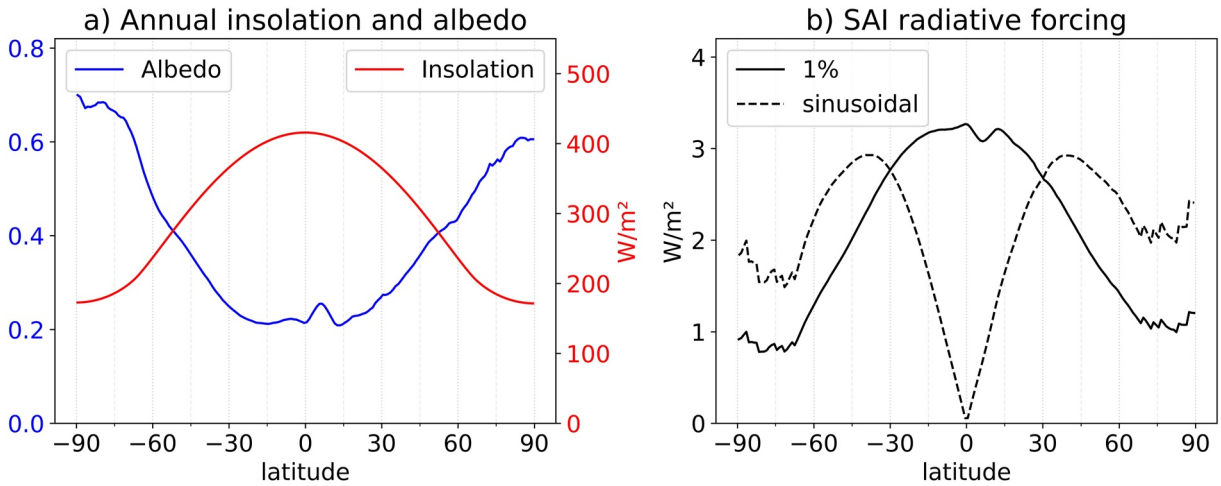


**Figure 2.** Idealized schematic of the potential for solar geoengineering radiative forcing by latitude. (a) zonally averaged annual mean top of atmosphere insolation ($W/m^2$), and zonally averaged annual mean albedo (no units). (b) zonally averaged annual mean top of atmosphere change in net shortwave flux ($W/m^2$) from a 1% reduction in insolation (solid line), and from a sinusoidal reduction in insolation growing from 0% at the Equator to 2% at the poles (dashed). The sinusoidal insolation reduction is designed to qualitatively match simulated stratospheric aerosol transport under polar SAI as shown in Figure 1b. Albedo and insolation are calculated from the NASA-CERES satellite data product over the period 2000–2020 (NASA/LARC/SD/ASDC., 2015). Shortwave forcings assume that SAI does not change tropospheric or surface albedo.

### 4.1. The Potential for SAI Forcing in the Polar Regions

The potential radiative forcing from SAI depends on both the local insolation and the top of atmosphere albedo. Stratospheric aerosols at high latitudes would have a smaller radiative forcing than at low latitudes because insolation is lower, and albedo is higher (Figure 2a). Annual mean insolation averaged over the regions poleward of 60° is approximately 45% of that at the Equator and the albedo in the polar regions is raised by the presence of ice and snow surfaces, and, in the Arctic, by extensive low level stratus clouds (Serreze et al., 2007). Arctic albedo peaks in the Spring, when sea ice and land snow cover are most extensive, and has a late-summer minimum (Sledd & L'Ecuyer, 2019). Considering seasonal variation in both insolation and albedo, we find that the local annual radiative forcing from a uniform reduction solar dimming is roughly 3 times larger in the tropics than in the polar regions (Figure 2b). A sinusoidal reduction in insolation which grows from zero at the Equator to peak at both poles, qualitatively similar in shape to that seen under high latitude SAI simulations produces a zonally integrated forcing which peaks in the mid-latitudes (Figure 2b).

Polar insolation is highly seasonal; the North Pole receives greater daily insolation than the Equator at the June solstice but receives essentially zero insolation through the winter months. As a result, in contrast to the situation at low latitudes, local instantaneous radiative forcing from polar SAI is strongly concentrated in summer, with negligible forcing in the winter months (Govindasamy & Caldeira, 2000). However, polar SAI can still impact the local climate during winter via changes to ocean heat uptake and sea ice during the sunlit seasons, and via changes to heat fluxes into the polar regions due to forcing from aerosols at lower latitudes (e.g., Moore et al., 2014).

Finally, we note that the path length through a layer of aerosols increases with higher zenith angle and thus with latitude. For example, if aerosols are uniformly distributed in a layer between 12 and 15 km altitude, and assuming a no-refracting spherical shell atmosphere, the path length through the aerosol layer is approximately 10 times greater at midwinter at 60°N than when the sun is directly overhead. This means that if measured as a fraction of incoming radiation, the depletion of the solar beam due to a uniform scattering layer is largest at high latitudes, and in winter (Lamb, 1970, p. ~462).

### 4.2. The Stratospheric Aerosol Distribution Under High Latitude Injection

The Brewer-Dobson circulation, which describes the mean meridional and vertical motions in the stratosphere, is characterized by rising in the tropics, poleward movement, and descent in the mid and high latitudes (Butchart, 2014). As a result, aerosols in the stratosphere are expected to spread polewards and to have a shorter lifetime if injected at high latitudes (Kravitz et al., 2017; Robock et al., 2008). The magnitude of this reduction

in aerosol lifetime depends on both the season of injection and its altitude (Toohey et al., 2019), and can be as great as a factor of four. For example, Robock et al. (2008) report an average lifetime of 3 months for injections at 68°N at 10–15 km altitude. This shorter lifetime means that the aerosol optical depth and local cooling per mass of sulfate injected under Arctic SAI is approximately doubled by limiting injection to the spring so that the aerosols are mostly present only during the sunlit months (W. R. Lee et al., 2021b). Maximizing the cooling per mass of injection would likely be advantageous, all else being equal, since it would reduce side effects such as sulfate deposition, as well as the cost of any implementation.

Model findings support the expectation that aerosols would spread polewards after injection, with various simulations showing maxima in aerosol concentrations at or near the pole (Jackson et al., 2015; W. R. Lee et al., 2021b, and see Figure 1). However, both models and observations of atmospheric tracers also show equatorward spread of high latitude injections (Figure 1). W. R. Lee et al. (2021b), Robock et al. (2008), and Jackson et al. (2015) model injection at 60°, 68° and 79°N, respectively, and all three studies find that the resulting aerosol distribution extends at relatively high concentrations to around 30°N before dropping off quickly toward the Equator. As a result of this stratospheric transport, in combination with the strong increase in annual mean insolation as latitude decreases, the zonally integrated shortwave radiative forcing from a polar SAI deployment can peak well equatorward of the injection latitude (W. R. Lee et al., 2023).

### 4.3. Cooling Efficiency of Polar SAI

Solar dimming experiments have found that large ($\gtrsim$10%) local reductions in insolation northwards of around 60°N would restore Arctic temperature under high emissions scenarios (Caldeira & Wood, 2008; MacCracken et al., 2013; Tilmes et al., 2014). To achieve the same restoration of Arctic sea ice or temperature, the percentage reduction in insolation required northwards of 60°N is approximately 4–5 times greater than the percentage global solar dimming (MacCracken et al., 2013; Tilmes et al., 2014). Larger local insolation reductions are required partly due to the lower absolute magnitude of insolation in the Arctic, but also because of local cloud feedbacks and compensatory northward heat fluxes. Tilmes et al. (2014) find that changes in Arctic clouds act to counteract local reductions in insolation, and several studies (Nalam et al., 2018; Tilmes et al., 2014) have shown that localized Arctic cooling raises the meridional temperature gradient, causing increased northward atmospheric heat fluxes.

Simulations of polar SAI also find that aerosol injection at high latitudes can restore Arctic (Jackson et al., 2015; W. R. Lee et al., 2021b, 2023; Nalam et al., 2018; Robock et al., 2008) and Antarctic (Nalam et al., 2018) temperatures. These SAI studies show a smaller difference in cooling efficiency between polar and global deployments than in solar dimming studies. W. R. Lee et al. (2023) report around 50% more Arctic cooling per unit mass injection at 60N than injection at low latitudes. Nalam et al. (2018) find an approximately equal Arctic cooling per unit mass, and less Antarctic cooling, when compared to a globally uniform stratospheric aerosol distribution.

Part of the explanation for the difference between SAI and solar dimming studies may lie in the significant radiative forcing from aerosols equatorward of the Arctic Circle in SAI simulations, expected given the latitudinal variation in insolation and albedo (see Figure 2). The maximum zonally integrated forcing in the Arctic SAI simulations of W. R. Lee et al. (2023) occurs well south of the injection latitude, at around 35°N. The resulting mid-latitude cooling then propagates to the Arctic via reduced northward heat fluxes; under a similar Arctic SAI scenario using the same model, W. R. Lee et al. (2021b) report compensatory heat fluxes which are an order of magnitude smaller than those found under one simulation of reduced insolation in only the region North of 60°N. Cooling efficiency is lower in the Antarctic than Arctic (Nalam et al., 2018), likely in part because the underlying albedo during local summer is higher in Antarctica due to the year-round land ice cover.

We now consider the cooling impact of polar SAI outside of the polar regions. Beginning again with the case of solar dimming, Caldeira and Wood (2008) show that global cooling is proportional to the area-integrated absolute reduction in insolation, that is, the reduction in solar energy input to the climate system, nearly independent of where that reduction occurs. This means that a very large reduction of ~50% in Arctic insolation (North of 71°N) is required to cool the whole planet by the same amount as a global reduction of 1%, due to the low insolation and high albedo of this region (see Figure 2). For SAI, four studies (W. R. Lee et al., 2023; Nalam et al., 2018; Robock et al., 2008; Sun et al., 2020) model both Arctic/polar SAI and tropical SAI. Across these four studies, polar SAI with spring-time injection appears to be less efficient at global cooling than low latitude SAI by a factor

of around 2 (see Table S2 in Supporting Information S1), where efficiency is defined as °C global cooling per unit sulfate injection. Were we to consider polar SAI with injection spread over the whole year rather than limited to the spring, we would expect the polar SAI efficiency to drop, by approximately another factor of 2 (W. R. Lee et al., 2021b), because the shorter aerosol lifetime in the high latitudes (Kravitz et al., 2017; Robock et al., 2008) means few particles injected in autumn and winter would survive to have a radiative impact in the following summer. Considering the spatial pattern of cooling across the globe, studies with Arctic only deployment consistently show patterns of cooling which peak at the pole and then reduce through the mid-latitudes to be close to zero in the opposite hemisphere (W. R. Lee et al., 2021b; W. R. Lee et al., 2023; Nalam et al., 2018), except in the case of very large Arctic injection magnitudes (100 Tg/year), for which significant cooling (∼1°C) has been simulated in the Southern Hemisphere (Sun et al., 2020).

### 4.4. Sea Ice and Arctic Hydrology Under Polar SAI

As polar-focused SAI would lower temperatures in the polar regions, it would offset many of the predominantly temperature driven climate impacts described in Section 3. Therefore, we do not now consider all these impacts, but will instead limit the discussion to sea ice and Arctic hydrology.

As was the case with global SAI (see Section 3.3), simulations show that with sufficiently large injection magnitudes, Arctic and Antarctic SAI can successfully restore summer sea ice to baseline levels under various high emissions pathways (Jackson et al., 2015; W. R. Lee et al., 2021b, 2023; Nalam et al., 2018). Restoration of sea ice using local SAI is more effective in local summer than winter (W. R. Lee et al., 2021b; Nalam et al., 2018). This difference is somewhat reduced for annual injection compared to spring only injection (W. R. Lee et al., 2021b; Nalam et al., 2018).

Localized polar insolation reductions have been found to increase latent heat flux into the polar regions (Nalam et al., 2018; Tilmes et al., 2014), resulting in precipitation increases in the Arctic and Antarctic relative both to pre-industrial and to a global solar dimming scenario (Nalam et al., 2018). In one simulation of Arctic insolation reduction under a high emissions scenario, while sea-ice volume is reduced by 34% compared to present, snow volume on the sea-ice is increased by approximately 50% (Tilmes et al., 2014). These precipitation changes raise the possibility that polar SAI might more effectively limit polar contributions to sea level rise than global SAI, since polar SAI might cool the Arctic and Antarctic while retaining part of the precipitation increases expected to increase accumulation on glaciers this century under warming scenarios (see Section 3.6). W. R. Lee et al. (2023) have conducted the only study yet to assess glacier surface mass balance (SMB) under polar SAI, although for Greenland only, and find that Arctic SAI is effective at restoring Greenland's SMB under future warming.

### 4.5. Global Precipitation Under Hemispheric SAI

While polar SAI could be hemispherically symmetric, various studies have simulated Arctic only deployments. In this section we assess the implications of the hemispherically asymmetric forcing implied by such scenarios on global rainfall. The Intertropical Convergence Zone (ITCZ) is a band of low pressure, deep convection, and heavy rainfall at the rising branch of the Hadley cell, near the equator. The ITCZ migrates toward the warmer hemisphere, both on seasonal timescales (Schneider et al., 2014), and on long timescales in the paleo-climate record (Koutavas & Lynch-Stieglitz, 2004). Simulations of hemispherically asymmetric stratospheric aerosol loadings similarly show displacement of the ITCZ toward the warmer hemisphere (Haywood et al., 2013; Nalam et al., 2018). This displacement is approximately linear in the annual mean interhemispheric temperature difference, moving approximately 0.6° latitude per degree Celsius (Nalam et al., 2018). Simulations of SAI with injections limited to one hemisphere show the impacts of such a displacement; under one SAI scenario with injections limited to the Northern Hemisphere, there is decreased rainfall in the regions of Africa and South America lying between approximately 0° and 10°N leading to net primary productivity reductions in the Sahel region of 60%–100% (Haywood et al., 2013). Under SAI with injection limited to the Southern Hemisphere, the opposite pattern is seen and widespread greening of the Sahel is observed, with net primary productivity increasing by over 100% (Haywood et al., 2013).

Simulations of SAI with injection limited to the Arctic region preferentially cool the Northern Hemisphere and, in the same manner as described above, they displace the ITCZ southwards (Jackson et al., 2015; W. R. Lee et al., 2023; Nalam et al., 2018; Sun et al., 2020). Jackson et al. (2015) simulate $SO_2$ injection over Svalbard

(78°55N) and generate a hemispheric cooling differential of approximately 1°C. This results in a substantial drying over the Sahel, Northern India, and parts of the Amazon. Qualitatively similar findings are consistent across Arctic SAI modeling. Simulations of SAI using multiple low-latitude injection sites commonly vary injection magnitudes to control for inter-hemispheric balance in order to avoid such tropical precipitation displacement (Kravitz et al., 2017; Richter et al., 2022; Tilmes et al., 2018) and similar hemispheric balancing appears possible for polar SAI (Nalam et al., 2018).

## 5. Polar Geoengineering Other Than SAI

### 5.1. Arctic Marine Cloud Brightening

Marine cloud brightening (MCB) is a proposal to increase the albedo of marine stratocumulus clouds to cool the planet. At global scales, modeling suggests spraying sea water droplets into a significant fraction of all marine stratocumulus clouds could produce a negative forcing of approximately the magnitude required to offset the warming from doubling $CO_2$ (Latham et al., 2008). The principal mechanism for this cooling is that aerosols act as additional cloud condensation nuclei, increasing the cloud droplet number concentration and thus the albedo (Twomey, 1974). Direct scattering of incoming radiation by the sprayed aerosols, and the increased lifetime of smaller cloud droplets also add to the modeled cooling (Ahlm et al., 2017).

Field-tests of MCB have recently been carried out as part of a project aiming to reduce extreme heat exposure for the Great Barrier Reef (Tollefson, 2021). A similar local use of MCB in the Arctic or Antarctic could be envisioned. Most studies of MCB have considered liquid-phase clouds (Wang et al., 2011), which contain no ice particles. However, mixed-phase clouds, which do contain ice particles, are common in the Arctic (Shupe, 2011). One study has evaluated the efficacy of marine cloud brightening in this mixed-phase, Arctic regime, and finds that while the presence of ice particles makes MCB less effective, it could still produce a significant negative local radiative forcing, estimated at 11 W/m$^2$ (Kravitz et al., 2014). However, Tilmes et al. (2014) report that a forcing more than an order of magnitude greater is required to preserve sea ice under the RCP8.5 scenario, if this forcing is limited to the region poleward of 60°N, in part due to compensatory poleward latent and specific heat fluxes. Such large local radiative forcings (on the order of 10% of insolation) have the potential to cause large land-sea temperature gradients, and associated hydrological changes (Kravitz et al., 2018). It is thought that the cost of global MCB might be broadly similar to that of global SAI, and therefore low compared to emissions mitigation and climate change damages (National Academies of Sciences, Engineering, and Medicine, 2021). No assessment exists in the literature of the expected costs or logistical feasibility of an Arctic or Antarctic MCB deployment.

### 5.2. Cirrus Cloud Thinning in the Polar Winter

Cirrus cloud thinning (CCT) is a proposal to increase the outgoing longwave radiation from the earth by thinning cirrus clouds in the upper troposphere (Gasparini & Lohmann, 2016; Mitchell & Finnegan, 2009; Storelvmo et al., 2013). Cirrus clouds have both a cooling effect on the climate, due to reflection of incoming shortwave radiation, and a warming effect, due to their absorption of outgoing longwave radiation and subsequent re-emission at lower temperature than the earth's surface. Globally, the warming effect is larger, and cirrus clouds have a net positive forcing of around 6 W/m$^2$ (Gasparini & Lohmann, 2016). As a result, reducing the optical thickness or extent of cirrus clouds globally would cool the planet, potentially with a magnitude similar to that of anthropogenic warming to date (Storelvmo & Herger, 2014).

CCT would involve seeding clouds with artificial ice nuclei in the hope that this would result in the growth of fewer, larger, ice crystals and thus decrease both the lifetime and optical depth of the cirrus clouds (Mitchell & Finnegan, 2009). Whether seeding would achieve such changes is uncertain (Gasparini & Lohmann, 2016; Penner et al., 2015), and warming due to counterproductive "overseeding" is also possible (Gasparini & Lohmann, 2016; Storelvmo et al., 2013; Storelvmo & Herger, 2014). However, if CCT is viable, it would be most effective in the polar regions during winter, since in these conditions, clouds have only the longwave warming effect, and no shortwave cooling, due to the lack of insolation (Storelvmo & Herger, 2014). Additionally, concentrations of natural ice nuclei are lowest in the high latitudes (especially the Southern Hemisphere), potentially making seeding more effective (Storelvmo & Herger, 2014).

Storelvmo and Herger (2014) find that CCT over only the high latitudes during winter (15% of the earth is seeded at any one time) results in a cooling of 1.4°C, as large as for global seeding. In addition, the cooling pattern produced peaks in the polar regions, and significant restoration of both Arctic and Antarctic sea ice is

modeled. However, a later version of the same model cannot reproduce these findings (Penner et al., 2015). Gruber et al. (2019) use a high-resolution process model to study cirrus cloud seeding over the Arctic during winter, and find that the seeding does successfully reduce ice crystal number concentrations, leading to cooling. Were CCT to be effective in the Arctic, it would be the only geoengineering method discussed here to generate a radiative forcing during the winter months, which is the time of strongest Arctic amplification of warming (Cohen et al., 2014).

### 5.3. Surface Albedo Modification of Sea Ice

It may be possible to increase the albedo of sea ice under specific conditions by covering it in a layer of tiny reflective glass spheres (Field et al., 2018). Some have therefore proposed a widespread deployment of such microspheres over Arctic sea ice to increase the albedo and thus increase sea-ice extent and volume (Field et al., 2018). However, while microspheres could brighten new ice (Field et al., 2018), which is typically thin and not snow covered, their non-zero absorbance means they may darken very high albedo surfaces, such as ice covered in thick snow. Webster and Warren (2022) consider the seasonal extents and spectral properties of the various surfaces present in the Arctic Ocean to show that the net effect of a uniform deployment of microspheres with ∼10% absorbance across the Arctic Ocean is a warming of the climate, with a positive radiative forcing of approximately 3 W/m$^2$ in the annual average. While significant albedo increases are modeled over new sea ice without snow cover, this is most extensive in the autumn and winter, when insolation is low, and as a result the radiative forcing achieved, while negative, is small (Webster & Warren, 2022).

Assuming it were possible to manufacture microspheres with perfect optical properties (i.e., with no absorbance), Webster and Warren (2022) find that an annual mean radiative forcing of approximately −3 W/m$^2$ over the Arctic could be achieved via a uniform deployment over all sea ice in May. This is likely more than an order of magnitude too small to preserve Arctic climate under a high emissions scenario (Tilmes et al., 2014), and, globally averaged, is approximately 1% of the anthropogenic radiative forcing at end-century under SSP5-8.5. It is not clear how logistics of such a deployment could be achieved. It would require annual spreading of $\sim 4 \times 10^{11}$ kg of microspheres (Webster & Warren, 2022). Assuming the density quoted by Field et al. (2018), this is $\sim 3 \times 10^{9}$ m$^3$ of microspheres, which is approximately 50% of 2021 global annual containerized trade by volume (CTAD, 2022). Only specialized ships can navigate the central Arctic, and Arctic shipping routes are currently open to ice-strengthened vessels for only several months in the late summer. Deployment via aircraft is unlikely to be viable due to the large volume of material required (Field et al., 2018).

## 6. Summary

SAI would be expected to cool the polar regions and to restore the polar climate and cryosphere toward its present state under future warming scenarios (Berdahl et al., 2014; Visioni, MacMartin, Kravitz, Boucher, et al., 2021). Simulations of SAI with low latitude or globally uniform injections generally under-cool the poles relative to the global mean, and thus see greater Arctic amplification and a greater change in the polar climate than under emissions mitigation only, at a given global temperature target (Berdahl et al., 2014; Ridley & Blockley, 2018). However, such polar under-cooling could likely be avoided with sufficient injection in the mid or high latitudes (Tilmes et al., 2018). There are only a small number of simulations of polar SAI, that is SAI with injections limited to regions of poleward of 60°. These simulations find that polar SAI would likely reduce change in polar climate somewhat more efficiently in terms of injection magnitude than global or low latitude injection, and would do so with less aerosol burden and cooling outside of the polar regions (W. R. Lee et al., 2021b; W. R. Lee et al., 2023; Nalam et al., 2018). Polar SAI, though, should still be considered a global, rather than regional, form of geoengineering. If injection was balanced across both hemispheres, all latitudes would see significant aerosol burdens and cooling (Section 4.2). Various studies have highlighted the important changes in tropical precipitation expected under an SAI deployment in one hemisphere only (see Section 4.5). This effect is not unique to polar SAI (Haywood et al., 2013) and modeling suggests it can be minimized by the balancing of injections across hemispheres (Kravitz et al., 2017; Richter et al., 2022; Tilmes et al., 2018). However, it does mean that a large Arctic-only SAI deployment may be undesirable due to the drying of Northern Hemisphere low-latitude regions which would be expected as a result (Jackson et al., 2015; W. R. Lee et al., 2023; Nalam et al., 2018; Sun et al., 2020).

There are various potential limitations in the ability of SAI to restore polar climate under global warming, as shown in Figure 3. First, since SAI only has a radiative forcing where there is sunlight to reflect, it cannot directly

10.1029/2023EF003679

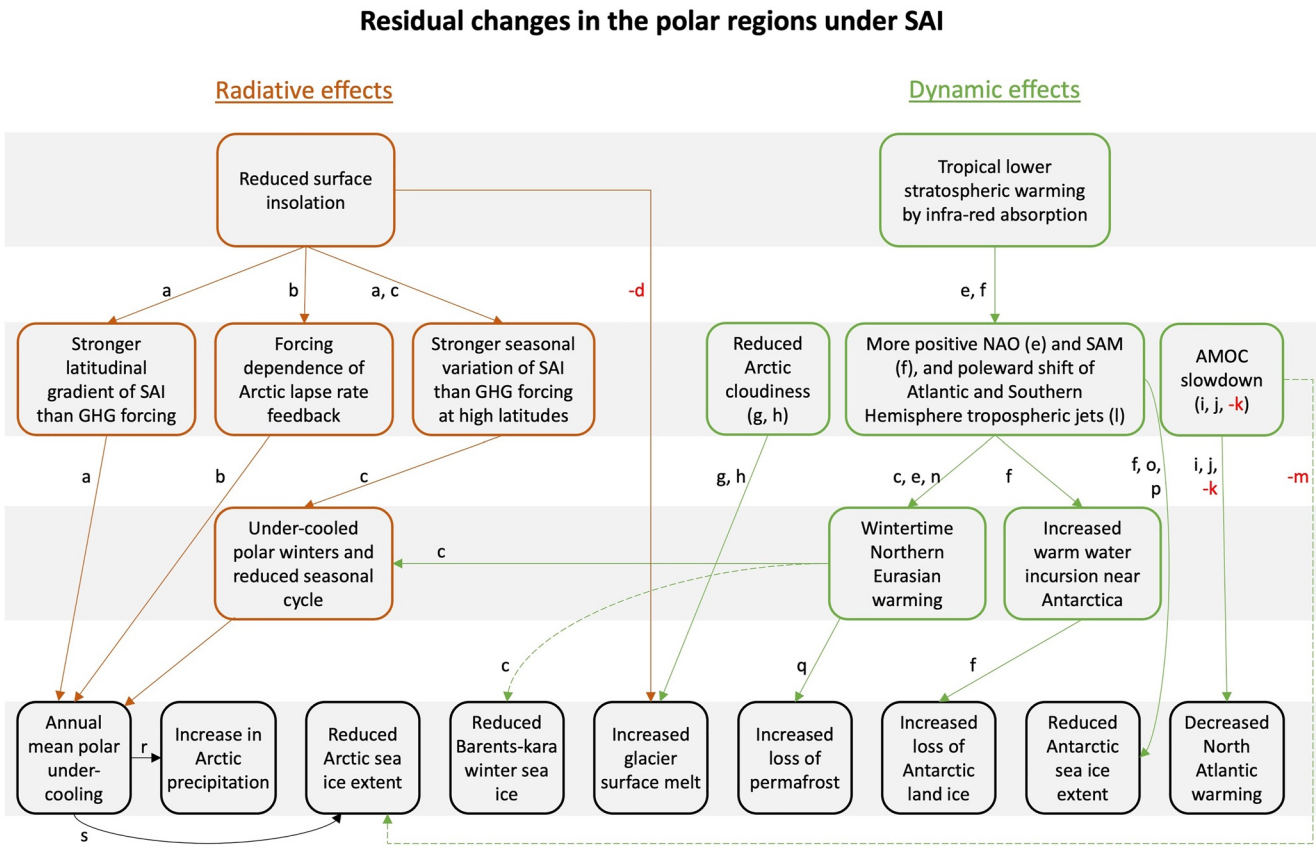


**Figure 3.** Schematic showing interactions resulting in residual changes in the polar regions under global SAI, relative to a world at the same global mean temperature without SAI. The figure does not show the first order effect of SAI, which is to cool the planet and reverse the effects of climate change; instead it only shows the residual changes. "Radiative effects" refer to mechanisms associated directly with the reduction in downward shortwave radiation at the surface caused by aerosol scattering. "Dynamic effects" refer to changes mediated by altered atmospheric and/or oceanic dynamics. Studies suggesting each mechanism are labeled by lowercase letters, with the references given in Table 2. Studies suggesting outcomes without a clear associated mechanism are labeled inside boxes. Letters in red prefaced with "–" signs indicate that the study suggests the opposite sign of change to that indicated in the box. Dashed lines indicate more tentative links, which are inferred without reference to an SAI modeling study.

cool the polar regions during the winter. In addition, stratospheric heating, which occurs as a side effect of SAI using sulfate particles, may cause winter-time warming over the high latitude Eurasian continent (Banerjee et al., 2021; A. Jones et al., 2021). Both effects contribute to an under-cooling, or even absolute warming in some regions, of the polar winter, and an associated suppression of the high latitude seasonal cycle (Jiang et al., 2019).

**Table 2**
*Studies Referenced in Figure 3*

| Label | Citation | Label (cont.) | Citation (cont.) |
|---|---|---|---|
| a | Govindasamy et al. (2003) | k | Fasullo et al. (2018) |
| b | Henry and Merlis (2020) | l | Simpson et al. (2019) |
| c | Jiang et al. (2019) | m | Mahajan et al. (2011) |
| d | Fettweis et al. (2021) | n | Banerjee et al. (2021) |
| e | A. Jones et al. (2021) | o | Zanchettin et al. (2014) |
| f | McCusker et al. (2015) | p | Coupe et al. (2023) |
| g | Moore et al. (2019) | q | Chen et al. (2023) |
| h | W.R. Lee et al. (2023) | r | Visioni, MacMartin, Kravitz, Boucher et al. (2021) |
| i | Xie et al. (2022) | s | Berdahl et al. (2014) |
| j | Fasullo and Richter (2023) | | |

Second, it is possible that a limited effectiveness of SAI to restore the Southern Ocean winds which drive upwelling of warm, deep waters around Antarctica might make SAI ineffective at preventing basal melting of ice shelves (McCusker et al., 2015), although this finding is as yet seen in only one model and the ocean circulation response to SAI is not consistent across versions of that model (Tilmes et al., 2020). This, in combination with the expected reduction in Antarctic precipitation under (low latitude) SAI relative to a warmer world (Visioni, MacMartin, Kravitz, Boucher, et al., 2021), raises the possibility that SAI could increase the Antarctic contribution to future sea level rise. Finally, localized cooling under polar SAI would cause changes to the atmospheric and oceanic meridional heat fluxes, with consequences including additional moisture flux into the polar regions (Nalam et al., 2018; Tilmes et al., 2014).

Marine cloud brightening and sea-ice albedo modification might produce a more localized polar cooling than SAI, but the limited evidence we have suggests that in both cases, the magnitude of this cooling would be insufficient to restore local climate under high emissions scenarios (Kravitz et al., 2014; Webster & Warren, 2022). Sea ice albedo modification appears unlikely to be capable of generating meaningful global climate impacts; the evidence reviewed above suggests that even in the best-case scenario, a marginal global cooling would be achieved via huge programmes of work requiring globally significant increases in manufacturing, shipping and $CO_2$ emissions. Further, there is a risk that sea-ice albedo modification with glass microspheres could actually decrease the surface albedo (Webster & Warren, 2022). Cirrus cloud thinning is the only known proposal for geoengineering with the potential to directly alter the radiative forcing during polar winter, and therefore if combined with SAI might offer a means of avoiding the suppression of the seasonal cycle discussed above. However, whether cirrus cloud thinning would generate a cooling as intended, globally or in the polar regions, is still highly uncertain (Gasparini & Lohmann, 2016).

## 7. Recommendations for Research

The study of the regional impacts of solar geoengineering, including on the polar regions, is a relatively novel research area, and there are major gaps in our understanding to be addressed before the polar response to this intervention in the climate system can be well characterized. Here, we have assessed simulations of SAI ranging from the simple, in which prescribed magnitudes of aerosol are simulated, to the more complex, in which aerosol magnitudes and injection latitudes are varied using a feedback control system to control features of the climate. We have also seen simulations with deployment at high latitudes. However, no simulation has combined these approaches to model SAI using a feedback control system while including high latitude injection as an available option to that control system. This simulation would be an obvious next step and could be used to test the ability of geoengineering with a polar component to simultaneously manage both polar and non-polar features of the climate system. Further, high latitude injection scenarios could usefully be included in future GeoMIP iterations, to test the inter-model variation in findings discussed in Section 4.

Various studies have assessed polar climate and changes in the cryosphere under SAI but, with one exception (Ridley & Blockley, 2018), these studies do not compare polar change under SAI with non-geoengineered scenarios at a particular global mean temperature. As a result, they do not allow a quantitative statement to be made of the relative efficacy of global SAI versus emissions mitigation in preserving polar climate. A future multi-model study using the GeoMIP G6sulfur simulations could test the robustness of the greater Arctic amplification under SAI reported by Ridley and Blockley (2018) across models. Such a study could contribute significantly to our understanding by quantifying the relative contributions to any polar under-cooling under SAI from insolation patterns, latitudinal albedo variation, stratospheric aerosol distribution and changes in atmospheric and oceanic heat fluxes.

The 20% increase in AMOC strength under the GLENS SAI scenario (Fasullo et al., 2018) and the residual southern ocean upwelling associated with basal melt of Antarctic ice sheets under SAI (McCusker et al., 2015) are findings with large implications for understanding the limitations of SAI in arresting change in the polar regions. Both findings are based on single model simulations, and are yet to be reproduced. As such a key research aim should be to, first, test whether these effects are present in other climate models, and second, develop the theoretical understanding of how variation in injection latitude might be expected to affect SAI's impact on these circulation changes.

## Data Availability Statement

Data for the GeoMIP simulations shown in Figure 1a can be downloaded from the Earth System Grid Federation CMIP6 archive (https://esgf-index1.ceda.ac.uk/search/cmip6-ceda/). Data for the high latitude stratospheric aerosol injection simulations shown in Figure 1b are available through the Cornell eCommons library (W. R. Lee et al., 2021a). The satellite data product for top of atmosphere albedo and insolation observations shown in Figure 2 can be downloaded from the NASA-CERES Atmospheric Science Data Store (NASA/LARC/SD/ASDC., 2015). All python code needed to recreate Figures 1 and 2 is publicly available in a repository on Zenodo (Duffey, 2023).

**Acknowledgments**
AD's contribution was funded by the London Natural Environment Research Council (NERC) Doctoral Training Partnership (DTP) Grant NE/S007229/1. MT acknowledges support from ESA (ESA/AO/1-9132/17/NL/MP and ESA/AO/1-10061/19/I-EF) and NERC (NE/T000546/1 and NE/X004643/1).

## References

Ahlm, L., Jones, A., Stjern, C. W., Muri, H., Kravitz, B., & Kristjánsson, J. E. (2017). Marine cloud brightening – As effective without clouds. *Atmospheric Chemistry and Physics*, *17*(21), 13071–13087. https://doi.org/10.5194/acp-17-13071-2017

Ammann, C. M., Washington, W. M., Meehl, G. A., Buja, L., & Teng, H. (2010). Climate engineering through artificial enhancement of natural forcings: Magnitudes and implied consequences. *Journal of Geophysical Research*, *115*(D22), D22109. https://doi.org/10.1029/2009JD012878

Aquila, V., Garfinkel, C. I., Newman, P., Oman, L., & Waugh, D. (2014). Modifications of the quasi-biennial oscillation by a geoengineering perturbation of the stratospheric aerosol layer. *Geophysical Research Letters*, *41*(5), 1738–1744. https://doi.org/10.1002/2013GL058818

Armstrong McKay, D. I., Staal, A., Abrams, J. F., Winkelmann, R., Sakschewski, B., Loriani, S., et al. (2022). Exceeding 1.5°C global warming could trigger multiple climate tipping points. *Science*, *377*(6611), eabn7950. https://doi.org/10.1126/science.abn7950

Bamber, J. L., Westaway, R. M., Marzeion, B., & Wouters, B. (2018). The land ice contribution to sea level during the satellite era. *Environmental Research Letters*, *13*(6), 063008. https://doi.org/10.1088/1748-9326/aac2f0

Banerjee, A., Butler, A. H., Polvani, L. M., Robock, A., Simpson, I. R., & Sun, L. (2021). Robust winter warming over Eurasia under stratospheric sulfate geoengineering – The role of stratospheric dynamics. *Atmospheric Chemistry and Physics*, *21*(9), 6985–6997. https://doi.org/10.5194/acp-21-6985-2021

Ban-Weiss, G. A., & Caldeira, K. (2010). Geoengineering as an optimization problem. *Environmental Research Letters*, *5*(3), 034009. https://doi.org/10.1088/1748-9326/5/3/034009

Bednarz, E. M., Visioni, D., Richter, J. H., Butler, A. H., & MacMartin, D. G. (2022). Impact of the latitude of stratospheric aerosol injection on the Southern Annular Mode. *Earth and Space Science Open Archive*. https://doi.org/10.1002/essoar.10511879.1

Bell, R. E., Banwell, A. F., Trusel, L. D., & Kingslake, J. (2018). Antarctic surface hydrology and impacts on ice-sheet mass balance. *Nature Climate Change*, *8*(12), 1044–1052. https://doi.org/10.1038/s41558-018-0326-3

Berdahl, M., Robock, A., Ji, D., Moore, J. C., Jones, A., Kravitz, B., & Watanabe, S. (2014). Arctic cryosphere response in the geoengineering model intercomparison project G3 and G4 scenarios. *Journal of Geophysical Research: Atmospheres*, *119*(3), 1308–1321. https://doi.org/10.1002/2013JD020627

Bintanja, R. (2018). The impact of Arctic warming on increased rainfall. *Scientific Reports*, *8*(1), 16001. https://doi.org/10.1038/s41598-018-34450-3

Bintanja, R., & Krikken, F. (2016). Magnitude and pattern of Arctic warming governed by the seasonality of radiative forcing. *Scientific Reports*, *6*(1), 38287. https://doi.org/10.1038/srep38287

Bintanja, R., & Selten, F. M. (2014). Future increases in Arctic precipitation linked to local evaporation and sea-ice retreat. *Nature*, *509*(7501), 479–482. https://doi.org/10.1038/nature13259

Biskaborn, B. K., Smith, S. L., Noetzli, J., Matthes, H., Vieira, G., Streletskiy, D. A., et al. (2019). Permafrost is warming at a global scale. *Nature Communications*, *10*(1), 264. https://doi.org/10.1038/s41467-018-08240-4

Burke, E. J., Zhang, Y., & Krinner, G. (2020). Evaluating permafrost physics in the Coupled Model Intercomparison Project 6 (CMIP6) models and their sensitivity to climate change. *The Cryosphere*, *14*(9), 3155–3174. https://doi.org/10.5194/tc-14-3155-2020

Butchart, N. (2014). The Brewer-Dobson circulation. *Reviews of Geophysics*, *52*(2), 157–184. https://doi.org/10.1002/2013RG000448

Caldeira, K., & Wood, L. (2008). Global and Arctic climate engineering: Numerical model studies. *Philosophical Transactions of the Royal Society A: Mathematical, Physical & Engineering Sciences*, *366*(1882), 4039–4056. https://doi.org/10.1098/rsta.2008.0132

Chadburn, S. E., Burke, E. J., Cox, P. M., Friedlingstein, P., Hugelius, G., & Westermann, S. (2017). An observation-based constraint on permafrost loss as a function of global warming. *Nature Climate Change*, *7*(5), 340–344. https://doi.org/10.1038/nclimate3262

Chen, Y., Ji, D., Zhang, Q., Moore, J. C., Boucher, O., Jones, A., et al. (2023). Northern-high-latitude permafrost and terrestrial carbon response to two solar geoengineering scenarios. *Earth System Dynamics*, *14*(1), 55–79. https://doi.org/10.5194/esd-14-55-2023

Chen, Y., Liu, A., & Moore, J. C. (2020). Mitigation of Arctic permafrost carbon loss through stratospheric aerosol geoengineering. *Nature Communications*, *11*(1), 2430. https://doi.org/10.1038/s41467-020-16357-8

Cohen, J., Screen, J. A., Furtado, J. C., Barlow, M., Whittleston, D., Coumou, D., et al. (2014). Recent Arctic amplification and extreme mid-latitude weather. *Nature Geoscience*, *7*(9), 627–637. https://doi.org/10.1038/ngeo2234

Comyn-Platt, E., Hayman, G., Huntingford, C., Chadburn, S. E., Burke, E. J., Harper, A. B., et al. (2018). Carbon budgets for 1.5 and 2°C targets lowered by natural wetland and permafrost feedbacks. *Nature Geoscience*, *11*(8), 568–573. https://doi.org/10.1038/s41561-018-0174-9

Coupe, J., Harrison, C., Robock, A., DuVivier, A., Maroon, E., Lovenduski, N. S., et al. (2023). Sudden reduction of Antarctic sea ice despite cooling after nuclear war. *Journal of Geophysical Research: Oceans*, *128*(1), e2022JC018774. https://doi.org/10.1029/2022JC018774

Coupe, J., & Robock, A. (2021). The influence of stratospheric soot and sulfate aerosols on the Northern Hemisphere wintertime atmospheric circulation. *Journal of Geophysical Research: Atmospheres*, *126*(11), e2020JD034513. https://doi.org/10.1029/2020JD034513

Cronin, T. W., & Jansen, M. F. (2016). Analytic radiative-advective equilibrium as a model for high-latitude climate. *Geophysical Research Letters*, *43*(1), 449–457. https://doi.org/10.1002/2015GL067172

CTAD, U. N. (2022). *Review of maritime transport 2022* (p. 195). REVIEW OF MARITIME TRANSPORT.

Dai, Z., Weisenstein, D. K., & Keith, D. W. (2018). Tailoring meridional and seasonal radiative forcing by sulfate aerosol solar geoengineering. *Geophysical Research Letters*, *45*(2), 1030–1039. https://doi.org/10.1002/2017GL076472

Day, J. J., Hargreaves, J. C., Annan, J. D., & Abe-Ouchi, A. (2012). Sources of multi-decadal variability in Arctic sea ice extent. *Environmental Research Letters*, *7*(3), 034011. https://doi.org/10.1088/1748-9326/7/3/034011

De, B., & Wu, Y. (2019). Robustness of the stratospheric pathway in linking the Barents-Kara Sea sea ice variability to the mid-latitude circulation in CMIP5 models. *Climate Dynamics*, *53*(1), 193–207. https://doi.org/10.1007/s00382-018-4576-6

DeConto, R. M., & Pollard, D. (2016). Contribution of Antarctica to past and future sea-level rise. *Nature*, *531*(7596), 591–597. https://doi.org/10.1038/nature17145

DeConto, R. M., Pollard, D., Alley, R. B., Velicogna, I., Gasson, E., Gomez, N., et al. (2021). The Paris Climate Agreement and future sea-level rise from Antarctica. *Nature*, *593*(7857), 83–89. https://doi.org/10.1038/s41586-021-03427-0

Desch, S. J., Smith, N., Groppi, C., Vargas, P., Jackson, R., Kalyaan, A., et al. (2017). Arctic ice management. *Earth's Future*, *5*(1), 107–127. https://doi.org/10.1002/2016EF000410

Duffey, A. (2023). Code for; solar geoengineering in the polar regions: A review. https://doi.org/10.5281/zenodo.7944258

Edwards, T. L., Nowicki, S., Marzeion, B., Hock, R., Goelzer, H., Seroussi, H., et al. (2021). Projected land ice contributions to twenty-first-century sea level rise. *Nature*, *593*(7857), 74–82. https://doi.org/10.1038/s41586-021-03302-y

Fasullo, J. T., & Richter, J. H. (2023). Dependence of strategic solar climate intervention on background scenario and model physics. *Atmospheric Chemistry and Physics*, *23*(1), 163–182. https://doi.org/10.5194/acp-23-163-2023

Fasullo, J. T., Tilmes, S., Richter, J. H., Kravitz, B., MacMartin, D. G., Mills, M. J., & Simpson, I. R. (2018). Persistent polar ocean warming in a strategically geoengineered climate. *Nature Geoscience*, *11*(12), 910–914. https://doi.org/10.1038/s41561-018-0249-7

Favier, L., Durand, G., Cornford, S. L., Gudmundsson, G. H., Gagliardini, O., Gillet-Chaulet, F., et al. (2014). Retreat of Pine Island glacier controlled by marine ice-sheet instability. *Nature Climate Change*, *4*(2), 117–121. https://doi.org/10.1038/nclimate2094

Fetterer, F., Knowles, K., Meier, W. N., Savoie, M., & Windnagel, A. K. (2017). *sea ice index, version 3*. NSIDC: National Snow and Ice Data Center. https://doi.org/10.7265/N5K072F8

Fettweis, X., Hofer, S., Séférian, R., Amory, C., Delhasse, A., Doutreloup, S., et al. (2021). Brief communication: Reduction in the future Greenland ice sheet surface melt with the help of solar geoengineering. *The Cryosphere*, *15*(6), 3013–3019. https://doi.org/10.5194/tc-15-3013-2021

Field, L., Ivanova, D., Bhattacharyya, S., Mlaker, V., Sholtz, A., Decca, R., et al. (2018). Increasing Arctic sea ice albedo using localized reversible geoengineering. *Earth's Future*, *6*(6), 882–901. https://doi.org/10.1029/2018EF000820

Fox-Kemper, B., Hewitt, H. T., Xiao, C., Aalgeirsdóttir, G., Drijfhout, S. S., Edwards, T. L., et al. (2021). Ocean, cryosphere, and sea level change. In V. Masson-Delmotte, et al. (Eds.). In *Climate change 2021: The physical science basis. Contribution of working group I to the sixth assessment report of the intergovernmental panel on climate change*. Cambridge University Press.

Francis, J. A., & Vavrus, S. J. (2012). Evidence linking Arctic amplification to extreme weather in mid-latitudes. *Geophysical Research Letters*, *39*(6). https://doi.org/10.1029/2012GL051000

Gasparini, B., & Lohmann, U. (2016). Why cirrus cloud seeding cannot substantially cool the planet. *Journal of Geophysical Research: Atmospheres*, *121*(9), 4877–4893. https://doi.org/10.1002/2015JD024666

Gasser, T., Kechiar, M., Ciais, P., Burke, E. J., Kleinen, T., Zhu, D., et al. (2018). Path-dependent reductions in $CO_2$ emission budgets caused by permafrost carbon release. *Nature Geoscience*, *11*(11), 830–835. https://doi.org/10.1038/s41561-018-0227-0

Goosse, H., Kay, J. E., Armour, K. C., Bodas-Salcedo, A., Chepfer, H., Docquier, D., et al. (2018). Quantifying climate feedbacks in polar regions. *Nature Communications*, *9*(1), 1919. https://doi.org/10.1038/s41467-018-04173-0

Govindasamy, B., & Caldeira, K. (2000). Geoengineering Earth's radiation balance to mitigate $CO_2$-induced climate change. *Geophysical Research Letters*, *27*(14), 2141–2144. https://doi.org/10.1029/1999GL006086

Govindasamy, B., Caldeira, K., & Duffy, P. B. (2003). Geoengineering Earth's radiation balance to mitigate climate change from a quadrupling of $CO_2$. *Global and Planetary Change*, *37*(1), 157–168. https://doi.org/10.1016/S0921-8181(02)00195-9

Gruber, S., Blahak, U., Haenel, F., Kottmeier, C., Leisner, T., Muskatel, H., et al. (2019). A process study on thinning of Arctic winter cirrus clouds with high-resolution ICON-ART simulations. *Journal of Geophysical Research: Atmospheres*, *124*(11), 5860–5888. https://doi.org/10.1029/2018JD029815

Gulev, S. K., Thorne, P. W., Ahn, J., Dentener, F. J., Domingues, C. M., Gerland, S., et al. (2021). *Changing state of the climate system*. In V. Masson-Delmotte et al. (Eds.), *Climate change 2021: The physical science basis. Contribution of working group I to the sixth assessment report of the intergovernmental panel on climate change*. Cambridge University Press. (Section: 2 Type: Book Section). Retrieved from https://www.ipcc.ch/report/ar6/wg1/downloads/report/IPCC_AR6_WGI_Chapter_02.pdf

Gutiérrez, J., Jones, R., Narisma, G., Alves, L., Amjad, M., Gorodetskaya, I., et al. (2021). Atlas. In V. Masson-Delmotte et al. (Eds.), In *Climate change 2021: The physical science basis. Contribution of working group I to the sixth assessment report of the intergovernmental panel on climate change* (pp. 1927–2058). Cambridge University Press. (Type: Book Section). https://doi.org/10.1017/9781009157896.021

Halstead, J. (2018). Stratospheric aerosol injection research and existential risk. *Futures*, *102*, 63–77. https://doi.org/10.1016/j.futures.2018.03.004

Haywood, J. M., Jones, A., Bellouin, N., & Stephenson, D. (2013). Asymmetric forcing from stratospheric aerosols impacts Sahelian rainfall. *Nature Climate Change*, *3*(7), 660–665. https://doi.org/10.1038/nclimate1857

Henry, M., & Merlis, T. M. (2020). Forcing dependence of atmospheric lapse rate changes dominates residual polar warming in solar radiation management climate scenarios. *Geophysical Research Letters*, *47*(15), e2020GL087929. https://doi.org/10.1029/2020GL087929

Henry, M., Merlis, T. M., Lutsko, N. J., & Rose, B. E. J. (2021). Decomposing the drivers of polar amplification with a single-column model. *Journal of Climate*, *34*(6), 2355–2365. https://doi.org/10.1175/JCLI-D-20-0178.1

Hoegh-Guldberg, O., Jacob, D., Bindi, M., Brown, S., Camilloni, I., Diedhiou, A., et al. (2018). Impacts of 1.5 C global warming on natural and human systems. Global warming of 1.5° C. (Publisher: IPCC Secretariat)

Hong, Y., Moore, J. C., Jevrejeva, S., Ji, D., Phipps, S. J., Lenton, A., et al. (2017). Impact of the GeoMIP G1 sunshade geoengineering experiment on the Atlantic meridional overturning circulation. *Environmental Research Letters*, *12*(3), 034009. https://doi.org/10.1088/1748-9326/aa5fb8

Horton, D. E., Johnson, N. C., Singh, D., Swain, D. L., Rajaratnam, B., & Diffenbaugh, N. S. (2015). Contribution of changes in atmospheric circulation patterns to extreme temperature trends. *Nature*, *522*(7557), 465–469. https://doi.org/10.1038/nature14550

IPCC. (2022). *Climate change 2022: Mitigation of climate change. Contribution of working group III to the sixth assessment report of the intergovernmental panel on climate change*. In P. Shukla, et al. (Eds.). Cambridge University Press. https://doi.org/10.1017/9781009157926

Irvine, P. J., & Keith, D. W. (2020). Halving warming with stratospheric aerosol geoengineering moderates policy-relevant climate hazards. *Environmental Research Letters*, *15*(4), 044011. https://doi.org/10.1088/1748-9326/ab76de

Irvine, P. J., Keith, D. W., & Moore, J. (2018). Brief communication: Understanding solar geoengineering's potential to limit sea level rise requires attention from cryosphere experts. *The Cryosphere*, *12*(7), 2501–2513. https://doi.org/10.5194/tc-12-2501-2018

Jackson, L. S., Crook, J. A., Jarvis, A., Leedal, D., Ridgwell, A., Vaughan, N., & Forster, P. M. (2015). Assessing the controllability of Arctic sea ice extent by sulfate aerosol geoengineering. *Geophysical Research Letters*, *42*(4), 1223–1231. https://doi.org/10.1002/2014GL062240

Jiang, J., Cao, L., MacMartin, D. G., Simpson, I. R., Kravitz, B., Cheng, W., et al. (2019). Stratospheric sulfate aerosol geoengineering could alter the high-latitude seasonal cycle. *Geophysical Research Letters*, *46*(23), 14153–14163. https://doi.org/10.1029/2019GL085758

Jones, A., Haywood, J. M., Alterskjær, K., Boucher, O., Cole, J. N. S., Curry, C. L., et al. (2013). The impact of abrupt suspension of solar radiation management (termination effect) in experiment G2 of the Geoengineering Model Intercomparison Project (GeoMIP). *Journal of Geophysical Research: Atmospheres*, *118*(17), 9743–9752. https://doi.org/10.1002/jgrd.50762

Jones, A., Haywood, J. M., Jones, A. C., Tilmes, S., Kravitz, B., & Robock, A. (2021). North Atlantic Oscillation response in GeoMIP experiments G6solar and G6sulfur: Why detailed modelling is needed for understanding regional implications of solar radiation management. *Atmospheric Chemistry and Physics*, *21*(2), 1287–1304. https://doi.org/10.5194/acp-21-1287-2021

Jones, A. C., Hawcroft, M. K., Haywood, J. M., Jones, A., Guo, X., & Moore, J. C. (2018). Regional climate impacts of stabilizing global warming at 1.5 K using solar geoengineering. *Earth's Future*, *6*(2), 230–251. https://doi.org/10.1002/2017EF000720

Joughin, I., Smith, B. E., & Medley, B. (2014). Marine ice sheet collapse potentially under way for the Thwaites Glacier Basin, West Antarctica. *Science*, *344*(6185), 735–738. https://doi.org/10.1126/science.1249055

Kashimura, H., Abe, M., Watanabe, S., Sekiya, T., Ji, D., Moore, J. C., et al. (2017). Shortwave radiative forcing, rapid adjustment, and feedback to the surface by sulfate geoengineering: Analysis of the geoengineering model intercomparison project G4 scenario. *Atmospheric Chemistry and Physics*, *17*(5), 3339–3356. https://doi.org/10.5194/acp-17-3339-2017

Koutavas, A., & Lynch-Stieglitz, J. (2004). Variability of the marine ITCZ over the Eastern Pacific during the past 30,000 years. In H. F. Diaz & R. S. Bradley (Eds.), *The Hadley circulation: Present, past and future* (pp. 347–369). Springer. https://doi.org/10.1007/978-1-4020-2944-8_13

Kravitz, B., Caldeira, K., Boucher, O., Robock, A., Rasch, P. J., Alterskjær, K., et al. (2013). Climate model response from the Geoengineering Model Intercomparison Project (GeoMIP). *Journal of Geophysical Research: Atmospheres*, *118*(15), 8320–8332. https://doi.org/10.1002/jgrd.50646

Kravitz, B., MacMartin, D. G., Mills, M. J., Richter, J. H., Tilmes, S., Lamarque, J.-F., et al. (2017). First simulations of designing stratospheric sulfate aerosol geoengineering to meet multiple simultaneous climate objectives. *Journal of Geophysical Research: Atmospheres*, *122*(23), 12616–12634. https://doi.org/10.1002/2017JD026874

Kravitz, B., MacMartin, D. G., Tilmes, S., Richter, J. H., Mills, M. J., Cheng, W., et al. (2019). Comparing surface and stratospheric impacts of geoengineering with different $SO_2$ injection strategies. *Journal of Geophysical Research: Atmospheres*, *124*(14), 7900–7918. https://doi.org/10.1029/2019JD030329

Kravitz, B., MacMartin, D. G., Wang, H., & Rasch, P. J. (2016). Geoengineering as a design problem. *Earth System Dynamics*, *7*(2), 469–497. https://doi.org/10.5194/esd-7-469-2016

Kravitz, B., Rasch, P. J., Wang, H., Robock, A., Gabriel, C., Boucher, O., et al. (2018). The climate effects of increasing ocean albedo: An idealized representation of solar geoengineering. *Atmospheric Chemistry and Physics*, *18*(17), 13097–13113. https://doi.org/10.5194/acp-18-13097-2018

Kravitz, B., Robock, A., Boucher, O., Schmidt, H., Taylor, K. E., Stenchikov, G., & Schulz, M. (2011). The Geoengineering Model Intercomparison Project (GeoMIP). *Atmospheric Science Letters*, *12*(2), 162–167. https://doi.org/10.1002/asl.316

Kravitz, B., Robock, A., Tilmes, S., Boucher, O., English, J. M., Irvine, P. J., et al. (2015). The geoengineering model intercomparison project phase 6 (GeoMIP6): Simulation design and preliminary results. *Geoscientific Model Development*, *8*(10), 3379–3392. https://doi.org/10.5194/gmd-8-3379-2015

Kravitz, B., Wang, H., Rasch, P. J., Morrison, H., & Solomon, A. B. (2014). Process-model simulations of cloud albedo enhancement by aerosols in the Arctic. *Philosophical Transactions of the Royal Society A: Mathematical, Physical & Engineering Sciences*, *372*(2031), 20140052. https://doi.org/10.1098/rsta.2014.0052

Kwok, R., & Rothrock, D. A. (2009). Decline in Arctic sea ice thickness from submarine and ICESat records: 1958–2008. *Geophysical Research Letters*, *36*(15). https://doi.org/10.1029/2009GL039035

Lamb, H. H. (1970). Volcanic dust in the atmosphere; with a chronology and assessment of its meteorological significance. *Philosophical Transactions of the Royal Society of London - Series A: Mathematical and Physical Sciences*, *266*(1178), 425–533. https://doi.org/10.1098/rsta.1970.0010

Latham, J., Gadian, A., Fournier, J., Parkes, B., Wadhams, P., & Chen, J. (2014). Marine cloud brightening: Regional applications. *Philosophical Transactions of the Royal Society A: Mathematical, Physical & Engineering Sciences*, *372*(2031), 20140053. https://doi.org/10.1098/rsta.2014.0053

Latham, J., Rasch, P., Chen, C.-C., Kettles, L., Gadian, A., Gettelman, A., et al. (2008). Global temperature stabilization via controlled albedo enhancement of low-level maritime clouds. *Philosophical Transactions of the Royal Society A: Mathematical, Physical & Engineering Sciences*, *366*(1882), 3969–3987. https://doi.org/10.1098/rsta.2008.0137

Lee, H., Ekici, A., Tjiputra, J., Muri, H., Chadburn, S. E., Lawrence, D. M., & Schwinger, J. (2019). The response of permafrost and high-latitude ecosystems under large-scale stratospheric aerosol injection and its termination. *Earth's Future*, *7*(6), 605–614. https://doi.org/10.1029/2018EF001146

Lee, W., MacMartin, D., Visioni, D., & Kravitz, B. (2020). Expanding the design space of stratospheric aerosol geoengineering to include precipitation-based objectives and explore trade-offs. *Earth System Dynamics*, *11*(4), 1051–1072. https://doi.org/10.5194/esd-11-1051-2020

Lee, W. R., MacMartin, D. G., Visioni, D., & Kravitz, B. (2021a). Data from: High-latitude stratospheric aerosol geoengineering may be more effective if injection is limited to spring. [Dataset]. https://doi.org/10.7298/d557-db75

Lee, W. R., MacMartin, D. G., Visioni, D., & Kravitz, B. (2021b). High-latitude stratospheric aerosol geoengineering can be more effective if injection is limited to spring. *Geophysical Research Letters*, *48*(9), e2021GL092696. https://doi.org/10.1029/2021GL092696

Lee, W. R., MacMartin, D. G., Visioni, D., Kravitz, B., Chen, Y., Moore, J. C., et al. (2023). High-latitude stratospheric aerosol injection to preserve the Arctic. *Earth's Future*, *11*(1), e2022EF003052. https://doi.org/10.1029/2022EF003052

Lenaerts, J. T. M., Vizcaino, M., Fyke, J., van Kampenhout, L., & van den Broeke, M. R. (2016). Present-day and future Antarctic ice sheet climate and surface mass balance in the Community Earth System Model. *Climate Dynamics*, *47*(5), 1367–1381. https://doi.org/10.1007/s00382-015-2907-4

Lenferna, G. A., Russotto, R. D., Tan, A., Gardiner, S. M., & Ackerman, T. P. (2017). Relevant climate response tests for stratospheric aerosol injection: A combined ethical and scientific analysis. *Earth's Future*, *5*(6), 577–591. https://doi.org/10.1002/2016EF000504

Lenton, T. M., Rockström, J., Gaffney, O., Rahmstorf, S., Richardson, K., Steffen, W., & Schellnhuber, H. J. (2019). Climate tipping points — Too risky to bet against. *Nature*, *575*(7784), 592–595. https://doi.org/10.1038/d41586-019-03595-0

Li, D., Zhang, R., & Knutson, T. (2018). Comparison of mechanisms for low-frequency variability of summer Arctic sea ice in three coupled models. *Journal of Climate*, *31*(3), 1205–1226. https://doi.org/10.1175/JCLI-D-16-0617.1

Li, D., Zhang, R., & Knutson, T. R. (2017). On the discrepancy between observed and CMIP5 multi-model simulated Barents Sea winter sea ice decline. *Nature Communications*, *8*(1), 14991. https://doi.org/10.1038/ncomms14991

Liu, A., Moore, J. C., & Chen, Y. (2023). PInc-PanTher estimates of Arctic permafrost soil carbon under the GeoMIP G6solar and G6sulfur experiments. *Earth System Dynamics*, *14*(1), 39–53. https://doi.org/10.5194/esd-14-39-2023

Lunt, D. J., Ridgwell, A., Valdes, P. J., & Seale, A. (2008). "Sunshade world": A fully coupled GCM evaluation of the climatic impacts of geoengineering. *Geophysical Research Letters*, *35*(12). https://doi.org/10.1029/2008GL033674
MacCracken, M. C. (2016). The rationale for accelerating regionally focused climate intervention research. *Earth's Future*, *4*(12), 649–657. https://doi.org/10.1002/2016EF000450
MacCracken, M. C., Shin, H.-J., Caldeira, K., & Ban-Weiss, G. A. (2013). Climate response to imposed solar radiation reductions in high latitudes. *Earth System Dynamics*, *4*(2), 301–315. https://doi.org/10.5194/esd-4-301-2013
MacDougall, A. H., Zickfeld, K., Knutti, R., & Matthews, H. D. (2015). Sensitivity of carbon budgets to permafrost carbon feedbacks and non-$CO_2$ forcings. *Environmental Research Letters*, *10*(12), 125003. https://doi.org/10.1088/1748-9326/10/12/125003
MacMartin, D. G., Keith, D. W., Kravitz, B., & Caldeira, K. (2013). Management of trade-offs in geoengineering through optimal choice of non-uniform radiative forcing. *Nature Climate Change*, *3*(4), 365–368. https://doi.org/10.1038/nclimate1722
MacMartin, D. G., & Kravitz, B. (2019). Mission-driven research for stratospheric aerosol geoengineering. *Proceedings of the National Academy of Sciences*, *116*(4), 1089–1094. https://doi.org/10.1073/pnas.1811022116
MacMynowski, D. G., Keith, D. W., Caldeira, K., & Shin, H.-J. (2011). Can we test geoengineering? *Energy & Environmental Science*, *4*(12), 5044–5052. https://doi.org/10.1039/C1EE01256H
Mahajan, S., Zhang, R., & Delworth, T. L. (2011). Impact of the Atlantic Meridional Overturning Circulation (AMOC) on Arctic surface air temperature and sea ice variability. *Journal of Climate*, *24*(24), 6573–6581. https://doi.org/10.1175/2011JCLI4002.1
Mallett, R. D. C., Stroeve, J. C., Cornish, S. B., Crawford, A. D., Lukovich, J. V., Serreze, M. C., et al. (2021). Record winter winds in 2020/21 drove exceptional Arctic sea ice transport. *Communications Earth & Environment*, *2*(1), 1–6. https://doi.org/10.1038/s43247-021-00221-8
Massom, R. A., Scambos, T. A., Bennetts, L. G., Reid, P., Squire, V. A., & Stammerjohn, S. E. (2018). Antarctic ice shelf disintegration triggered by sea ice loss and ocean swell. *Nature*, *558*(7710), 383–389. https://doi.org/10.1038/s41586-018-0212-1
McCrystall, M. R., Stroeve, J., Serreze, M., Forbes, B. C., & Screen, J. A. (2021). New climate models reveal faster and larger increases in Arctic precipitation than previously projected. *Nature Communications*, *12*(1), 6765. https://doi.org/10.1038/s41467-021-27031-y
McCusker, K. E., Battisti, D. S., & Bitz, C. M. (2015). Inability of stratospheric sulfate aerosol injections to preserve the West Antarctic Ice Sheet. *Geophysical Research Letters*, *42*(12), 4989–4997. https://doi.org/10.1002/2015GL064314
Mitchell, D. L., & Finnegan, W. (2009). Modification of cirrus clouds to reduce global warming. *Environmental Research Letters*, *4*(4), 045102. https://doi.org/10.1088/1748-9326/4/4/045102
Moore, J. C., Gladstone, R., Zwinger, T., & Wolovick, M. (2018). Geoengineer polar glaciers to slow sea-level rise. *Nature*, *555*(7696), 303–305. https://doi.org/10.1038/d41586-018-03036-4
Moore, J. C., Rinke, A., Yu, X., Ji, D., Cui, X., Li, Y., et al. (2014). Arctic sea ice and atmospheric circulation under the GeoMIP G1 scenario. *Journal of Geophysical Research: Atmospheres*, *119*(2), 567–583. https://doi.org/10.1002/2013JD021060
Moore, J. C., Yue, C., Zhao, L., Guo, X., Watanabe, S., & Ji, D. (2019). Greenland ice sheet response to stratospheric aerosol injection geoengineering. *Earth's Future*, *7*(12), 1451–1463. https://doi.org/10.1029/2019EF001393
Moriyama, R., Sugiyama, M., Kurosawa, A., Masuda, K., Tsuzuki, K., & Ishimoto, Y. (2017). The cost of stratospheric climate engineering revisited. *Mitigation and Adaptation Strategies for Global Change*, *22*(8), 1207–1228. https://doi.org/10.1007/s11027-016-9723-y
Mottram, R., Hansen, N., Kittel, C., van Wessem, J. M., Agosta, C., Amory, C., et al. (2021). What is the surface mass balance of Antarctica? An intercomparison of regional climate model estimates. *The Cryosphere*, *15*(8), 3751–3784. https://doi.org/10.5194/tc-15-3751-2021
Mudryk, L., Santolaria-Otín, M., Krinner, G., Ménégoz, M., Derksen, C., Brutel-Vuilmet, C., et al. (2020). Historical Northern Hemisphere snow cover trends and projected changes in the CMIP6 multi-model ensemble. *The Cryosphere*, *14*(7), 2495–2514. https://doi.org/10.5194/tc-14-2495-2020
Nalam, A., Bala, G., & Modak, A. (2018). Effects of Arctic geoengineering on precipitation in the tropical monsoon regions. *Climate Dynamics*, *50*(9), 3375–3395. https://doi.org/10.1007/s00382-017-3810-y
NASA/LARC/SD/ASDC. (2015). CERES time-interpolated TOA fluxes, clouds and aerosols monthly Terra Edition4A. [Dataset]. NASA Langley Atmospheric Science Data Center DAAC. https://doi.org/10.5067/TERRA/CERES/SSF1DEGMONTH_L3.004A
National Academies of Sciences, Engineering, and Medicine. (2021). *Reflecting sunlight: Recommendations for solar geoengineering research and research governance*. The National Academies Press. https://doi.org/10.17226/25762
Notz, D., & Community, S. (2020). Arctic sea ice in CMIP6. *Geophysical Research Letters*, *47*(10), e2019GL086749. https://doi.org/10.1029/2019GL086749
Notz, D., & Stroeve, J. (2016). Observed Arctic sea-ice loss directly follows anthropogenic $CO_2$ emission. *Science*, *354*(6313), 747–750. https://doi.org/10.1126/science.aag2345
Notz, D., & Stroeve, J. (2018). The trajectory towards a seasonally ice-free Arctic Ocean. *Current Climate Change Reports*, *4*(4), 407–416. https://doi.org/10.1007/s40641-018-0113-2
Overland, J. E., Dethloff, K., Francis, J. A., Hall, R. J., Hanna, E., Kim, S.-J., et al. (2016). Nonlinear response of mid-latitude weather to the changing Arctic. *Nature Climate Change*, *6*(11), 992–999. https://doi.org/10.1038/nclimate3121
Pattyn, F., Ritz, C., Hanna, E., Asay-Davis, X., DeConto, R., Durand, G., et al. (2018). The Greenland and Antarctic ice sheets under 1.5°C global warming. *Nature Climate Change*, *8*(12), 1053–1061. https://doi.org/10.1038/s41558-018-0305-8
Pauling, A. G., Bushuk, M., & Bitz, C. M. (2021). Robust inter-hemispheric asymmetry in the response to symmetric volcanic forcing in model large ensembles. *Geophysical Research Letters*, *48*(9), e2021GL092558. https://doi.org/10.1029/2021GL092558
Penner, J. E., Zhou, C., & Liu, X. (2015). Can cirrus cloud seeding be used for geoengineering? *Geophysical Research Letters*, *42*(20), 8775–8782. https://doi.org/10.1002/2015GL065992
Pistone, K., Eisenman, I., & Ramanathan, V. (2014). Observational determination of albedo decrease caused by vanishing Arctic sea ice. *Proceedings of the National Academy of Sciences*, *111*(9), 3322–3326. https://doi.org/10.1073/pnas.1318201111
Pithan, F., & Jung, T. (2021). Arctic amplification of precipitation changes—The energy hypothesis. *Geophysical Research Letters*, *48*(21), e2021GL094977. https://doi.org/10.1029/2021GL094977
Pithan, F., & Mauritsen, T. (2014). Arctic amplification dominated by temperature feedbacks in contemporary climate models. *Nature Geoscience*, *7*(3), 181–184. https://doi.org/10.1038/ngeo2071
Pollard, D., DeConto, R. M., & Alley, R. B. (2015). Potential Antarctic Ice Sheet retreat driven by hydrofracturing and ice cliff failure. *Earth and Planetary Science Letters*, *412*, 112–121. https://doi.org/10.1016/j.epsl.2014.12.035
Polvani, L. M., Banerjee, A., & Schmidt, A. (2019). Northern Hemisphere continental winter warming following the 1991 Mt. Pinatubo eruption: Reconciling models and observations. *Atmospheric Chemistry and Physics*, *19*(9), 6351–6366. https://doi.org/10.5194/acp-19-6351-2019
Pörtner, H.-O., Roberts, D., Masson-Delmotte, V., & Zhai, P. (2019). IPCC special report on the ocean and cryosphere in a changing climate (Technical report). Retrieved from https://www.ipcc.ch/srocc/

Pritchard, H. D., Ligtenberg, S. R. M., Fricker, H. A., Vaughan, D. G., van den Broeke, M. R., & Padman, L. (2012). Antarctic ice-sheet loss driven by basal melting of ice shelves. *Nature*, *484*(7395), 502–505. https://doi.org/10.1038/nature10968

Rantanen, M., Karpechko, A. Y., Lipponen, A., Nordling, K., Hyvärinen, O., Ruosteenoja, K., et al. (2022). The Arctic has warmed nearly four times faster than the globe since 1979. *Communications Earth & Environment*, *3*(1), 1–10. https://doi.org/10.1038/s43247-022-00498-3

Richter, J. H., Visioni, D., MacMartin, D. G., Bailey, D. A., Rosenbloom, N., Dobbins, B., et al. (2022). Assessing responses and impacts of solar climate intervention on the Earth system with stratospheric aerosol injection (ARISE-SAI): Protocol and initial results from the first simulations. *Geoscientific Model Development*, *15*(22), 8221–8243. https://doi.org/10.5194/gmd-15-8221-2022

Ridley, J. K., & Blockley, E. W. (2018). Brief communication: Solar radiation management not as effective as $CO_2$ mitigation for Arctic sea ice loss in hitting the 1.5 and 2°C COP climate targets. *The Cryosphere*, *12*(10), 3355–3360. https://doi.org/10.5194/tc-12-3355-2018

Rignot, E., Mouginot, J., Scheuchl, B., van den Broeke, M., van Wessem, M. J., & Morlighem, M. (2019). Four decades of Antarctic Ice Sheet mass balance from 1979–2017. *Proceedings of the National Academy of Sciences*, *116*(4), 1095–1103. https://doi.org/10.1073/pnas.1812883116

Rigor, I. G., Wallace, J. M., & Colony, R. L. (2002). Response of sea ice to the Arctic oscillation. *Journal of Climate*, *15*(18), 2648–2663. https://doi.org/10.1175/1520-0442(2002)015⟨2648:ROSITT⟩2.0.CO;2

Robock, A. (2000). Volcanic eruptions and climate. *Reviews of Geophysics*, *38*(2), 191–219. https://doi.org/10.1029/1998RG000054

Robock, A., Oman, L., & Stenchikov, G. L. (2008). Regional climate responses to geoengineering with tropical and Arctic $SO_2$ injections. *Journal of Geophysical Research*, *113*(D16), D16101. https://doi.org/10.1029/2008JD010050

Russotto, R. D., & Biasutti, M. (2020). Polar amplification as an inherent response of a circulating atmosphere: Results from the TRACMIP aquaplanets. *Geophysical Research Letters*, *47*(6), e2019GL086771. https://doi.org/10.1029/2019GL086771

Schneider, T., Bischoff, T., & Haug, G. H. (2014). Migrations and dynamics of the intertropical convergence zone. *Nature*, *513*(7516), 45–53. https://doi.org/10.1038/nature13636

Schuur, E. A. G., Abbott, B. W., Commane, R., Ernakovich, J., Euskirchen, E., Hugelius, G., et al. (2022). Permafrost and climate change: Carbon cycle feedbacks from the warming Arctic. *Annual Review of Environment and Resources*, *47*(1), 343–371. https://doi.org/10.1146/annurev-environ-012220-011847

Seroussi, H., Nowicki, S., Payne, A. J., Goelzer, H., Lipscomb, W. H., Abe-Ouchi, A., et al. (2020). ISMIP6 Antarctica: A multi-model ensemble of the Antarctic ice sheet evolution over the 21st century. *The Cryosphere*, *14*(9), 3033–3070. https://doi.org/10.5194/tc-14-3033-2020

Serreze, M. C., Barrett, A. P., Slater, A. G., Steele, M., Zhang, J., & Trenberth, K. E. (2007). The large-scale energy budget of the Arctic. *Journal of Geophysical Research*, *112*(D11), D11122. https://doi.org/10.1029/2006JD008230

Shepherd, J. G. (2009). *Geoengineering the climate: Science, governance and uncertainty*. Royal Society. Retrieved from https://eprints.soton.ac.uk/156647/

Shindell, D. T., Schmidt, G. A., Mann, M. E., & Faluvegi, G. (2004). Dynamic winter climate response to large tropical volcanic eruptions since 1600. *Journal of Geophysical Research*, *109*(D5), D05104. https://doi.org/10.1029/2003JD004151

Shupe, M. D. (2011). Clouds at Arctic atmospheric observatories. Part II: Thermodynamic phase characteristics. *Journal of Applied Meteorology and Climatology*, *50*(3), 645–661. https://doi.org/10.1175/2010JAMC2468.1

Siegert, M., Atkinson, A., Banwell, A., Brandon, M., Convey, P., Davies, B., et al. (2019). The Antarctic Peninsula under a 1.5°C global warming scenario. *Frontiers in Environmental Science*, *7*. https://doi.org/10.3389/fenvs.2019.00102

Simpkins, G. (2021). Breaking down the NAO–AO connection. *Nature Reviews Earth & Environment*, *2*(2), 88. https://doi.org/10.1038/s43017-021-00139-x

Simpson, I. R., Tilmes, S., Richter, J. H., Kravitz, B., MacMartin, D. G., Mills, M. J., et al. (2019). The regional hydroclimate response to stratospheric sulfate geoengineering and the role of stratospheric heating. *Journal of Geophysical Research: Atmospheres*, *124*(23), 12587–12616. https://doi.org/10.1029/2019JD031093

Sledd, A., & L'Ecuyer, T. (2019). How much do clouds mask the impacts of Arctic sea ice and snow cover variations? Different perspectives from observations and reanalyses. *Atmosphere*, *10*(1), 12. https://doi.org/10.3390/atmos10010012

Smith, W. (2020). The cost of stratospheric aerosol injection through 2100. *Environmental Research Letters*, *15*(11), 114004. https://doi.org/10.1088/1748-9326/aba7e7

Smith, W., Bhattarai, U., MacMartin, D. G., Lee, W. R., Visioni, D., Kravitz, B., & Rice, C. V. (2022). A subpolar-focused stratospheric aerosol injection deployment scenario. *Environmental Research Communications*, *4*(9), 095009. https://doi.org/10.1088/2515-7620/ac8cd3

Sognnaes, I., Gambhir, A., van de Ven, D.-J., Nikas, A., Anger-Kraavi, A., Bui, H., et al. (2021). A multi-model analysis of long-term emissions and warming implications of current mitigation efforts. *Nature Climate Change*, *11*(12), 1055–1062. https://doi.org/10.1038/s41558-021-01206-3

Storelvmo, T., & Herger, N. (2014). Cirrus cloud susceptibility to the injection of ice nuclei in the upper troposphere. *Journal of Geophysical Research: Atmospheres*, *119*(5), 2375–2389. https://doi.org/10.1002/2013JD020816

Storelvmo, T., Kristjansson, J. E., Muri, H., Pfeffer, M., Barahona, D., & Nenes, A. (2013). Cirrus cloud seeding has potential to cool climate. *Geophysical Research Letters*, *40*(1), 178–182. https://doi.org/10.1029/2012GL054201

Stroeve, J. C., Maslanik, J., Serreze, M. C., Rigor, I., Meier, W., & Fowler, C. (2011). Sea ice response to an extreme negative phase of the Arctic Oscillation during winter 2009/2010. *Geophysical Research Letters*, *38*(2). https://doi.org/10.1029/2010GL045662

Sun, W., Wang, B., Chen, D., Gao, C., Lu, G., & Liu, J. (2020). Global monsoon response to tropical and Arctic stratospheric aerosol injection. *Climate Dynamics*, *55*(7), 2107–2121. https://doi.org/10.1007/s00382-020-05371-7

Tewari, K., Mishra, S. K., Salunke, P., & Dewan, A. (2022). Future projections of temperature and precipitation for Antarctica. *Environmental Research Letters*, *17*(1), 014029. https://doi.org/10.1088/1748-9326/ac43e2

The IMBIE Team. (2018). Mass balance of the Antarctic Ice Sheet from 1992 to 2017. *Nature*, *558*(7709), 219–222. https://doi.org/10.1038/s41586-018-0179-y

The IMBIE Team. (2020). Mass balance of the Greenland Ice Sheet from 1992 to 2018. *Nature*, *579*(7798), 233–239. https://doi.org/10.1038/s41586-019-1855-2

Thoma, M., Jenkins, A., Holland, D., & Jacobs, S. (2008). Modelling circumpolar deep water intrusions on the Amundsen Sea continental shelf, Antarctica. *Geophysical Research Letters*, *35*(18), L18602. https://doi.org/10.1029/2008GL034939

Thompson, D. W. J., & Wallace, J. M. (2001). Regional climate impacts of the Northern Hemisphere annular mode. *Science*, *293*(5527), 85–89. https://doi.org/10.1126/science.1058958

Tilmes, S., Jahn, A., Kay, J. E., Holland, M., & Lamarque, J.-F. (2014). Can regional climate engineering save the summer Arctic sea ice? *Geophysical Research Letters*, *41*(3), 880–885. https://doi.org/10.1002/2013GL058731

Tilmes, S., MacMartin, D. G., Lenaerts, J. T. M., van Kampenhout, L., Muntjewerf, L., Xia, L., et al. (2020). Reaching 1.5 and 2.0°C global surface temperature targets using stratospheric aerosol geoengineering. *Earth System Dynamics*, *11*(3), 579–601. https://doi.org/10.5194/esd-11-579-2020

Tilmes, S., Richter, J. H., Kravitz, B., MacMartin, D. G., Mills, M. J., Simpson, I. R., et al. (2018). CESM1(WACCM) stratospheric aerosol geoengineering large ensemble project. *Bulletin of the American Meteorological Society*, *99*(11), 2361–2371. https://doi.org/10.1175/BAMS-D-17-0267.1

Tollefson, J. (2021). Can artificially altered clouds save the Great Barrier Reef? *Nature*, *596*(7873), 476–478. https://doi.org/10.1038/d41586-021-02290-3

Toohey, M., Krüger, K., Schmidt, H., Timmreck, C., Sigl, M., Stoffel, M., & Wilson, R. (2019). Disproportionately strong climate forcing from extratropical explosive volcanic eruptions. *Nature Geoscience*, *12*(2), 100–107. https://doi.org/10.1038/s41561-018-0286-2

Turner, J., Bracegirdle, T. J., Phillips, T., Marshall, G. J., & Hosking, J. S. (2013). An initial assessment of Antarctic sea ice extent in the CMIP5 models. *Journal of Climate*, *26*(5), 1473–1484. https://doi.org/10.1175/JCLI-D-12-00068.1

Twomey, S. (1974). Pollution and the planetary albedo. *Atmospheric Environment*, *8*(12), 1251–1256. https://doi.org/10.1016/0004-6981(74)90004-3

UN Environment Programme. (2022). Emissions gap report 2022. Retrieved from https://www.unep.org/resources/emissions-gap-report-2022

UNFCCC. (2015). Adoption of the Paris Agreement. Report No. FCCC/CP/2015/L.9/Rev.1. Retrieved from http://unfccc.int/resource/docs/2015/cop21/eng/l09r01.pdf

van de Ven, D. J., Mittal, S., Gambhir, A., Lamboll, R. D., Doukas, H., Giarola, S., et al. (2023). A multimodel analysis of post-Glasgow climate targets and feasibility challenges. *Nature Climate Change*, 1–9. https://doi.org/10.1038/s41558-023-01661-0

van den Broeke, M., Bamber, J., Ettema, J., Rignot, E., Schrama, E., van de Berg, W. J., et al. (2009). Partitioning recent Greenland mass loss. *Science*, *326*(5955), 984–986. https://doi.org/10.1126/science.1178176

Verona, L. S., Wainer, I., & Stevenson, S. (2019). Volcanically triggered ocean warming near the Antarctic Peninsula. *Scientific Reports*, *9*(1), 9462. https://doi.org/10.1038/s41598-019-45190-3

Visioni, D., Kravitz, B., Robock, A., Tilmes, S., Haywood, J., Boucher, O., et al. (2023). Opinion: The scientific and community-building roles of the Geoengineering Model Intercomparison Project (GeoMIP) – Past, present, and future. *Atmospheric Chemistry and Physics*, *23*(9), 5149–5176. https://doi.org/10.5194/acp-23-5149-2023

Visioni, D., MacMartin, D. G., & Kravitz, B. (2021). Is turning down the sun a good proxy for stratospheric sulfate geoengineering? *Journal of Geophysical Research: Atmospheres*, *126*(5), e2020JD033952. https://doi.org/10.1029/2020JD033952

Visioni, D., MacMartin, D. G., Kravitz, B., Boucher, O., Jones, A., Lurton, T., et al. (2021). Identifying the sources of uncertainty in climate model simulations of solar radiation modification with the G6sulfur and G6solar Geoengineering Model Intercomparison Project (GeoMIP) simulations. *Atmospheric Chemistry and Physics*, *21*(13), 10039–10063. https://doi.org/10.5194/acp-21-10039-2021

Visioni, D., MacMartin, D. G., Kravitz, B., Richter, J. H., Tilmes, S., & Mills, M. J. (2020). Seasonally modulated stratospheric aerosol geoengineering alters the climate outcomes. *Geophysical Research Letters*, *47*(12), e2020GL088337. https://doi.org/10.1029/2020GL088337

Wang, H., Rasch, P. J., & Feingold, G. (2011). Manipulating marine stratocumulus cloud amount and albedo: A process-modelling study of aerosol-cloud-precipitation interactions in response to injection of cloud condensation nuclei. *Atmospheric Chemistry and Physics*, *11*(9), 4237–4249. https://doi.org/10.5194/acp-11-4237-2011

Webster, M. A., & Warren, S. G. (2022). Regional geoengineering using tiny glass bubbles would accelerate the loss of Arctic sea ice. *Earth's Future*, *10*(10), e2022EF002815. https://doi.org/10.1029/2022EF002815

Wunderlich, F., & Mitchell, D. M. (2017). Revisiting the observed surface climate response to large volcanic eruptions. *Atmospheric Chemistry and Physics*, *17*(1), 485–499. https://doi.org/10.5194/acp-17-485-2017

Xie, M., Moore, J. C., Zhao, L., Wolovick, M., & Muri, H. (2022). Impacts of three types of solar geoengineering on the Atlantic meridional overturning circulation. *Atmospheric Chemistry and Physics*, *22*(7), 4581–4597. https://doi.org/10.5194/acp-22-4581-2022

Xu, K.-M., & Emanuel, K. A. (1989). Is the tropical atmosphere conditionally unstable? *Monthly Weather Review*, *117*(7), 1471–1479. https://doi.org/10.1175/1520-0493(1989)117⟨1471:ITTACU⟩2.0.CO;2

Yang, W., & Magnusdottir, G. (2018). Year-to-year variability in Arctic minimum sea ice extent and its preconditions in observations and the CESM large ensemble simulations. *Scientific Reports*, *8*(1), 9070. https://doi.org/10.1038/s41598-018-27149-y

Yeager, S. G., Karspeck, A. R., & Danabasoglu, G. (2015). Predicted slowdown in the rate of Atlantic sea ice loss. *Geophysical Research Letters*, *42*(24), 10704–10713. https://doi.org/10.1002/2015GL065364

Yu, X., Moore, J. C., Cui, X., Rinke, A., Ji, D., Kravitz, B., & Yoon, J.-H. (2015). Impacts, effectiveness and regional inequalities of the GeoMIP G1 to G4 solar radiation management scenarios. *Global and Planetary Change*, *129*, 10–22. https://doi.org/10.1016/j.gloplacha.2015.02.010

Zanchettin, D., Bothe, O., Timmreck, C., Bader, J., Beitsch, A., Graf, H.-F., et al. (2014). Inter-hemispheric asymmetry in the sea-ice response to volcanic forcing simulated by MPI-ESM (COSMOS-Mill). *Earth System Dynamics*, *5*(1), 223–242. https://doi.org/10.5194/esd-5-223-2014

Zhang, R. (2015). Mechanisms for low-frequency variability of summer Arctic sea ice extent. *Proceedings of the National Academy of Sciences*, *112*(15), 4570–4575. https://doi.org/10.1073/pnas.1422296112

Zhang, Y., MacMartin, D. G., Visioni, D., & Kravitz, B. (2022). How large is the design space for stratospheric aerosol geoengineering? *Earth System Dynamics*, *13*(1), 201–217. https://doi.org/10.5194/esd-13-201-2022